

Supporting Information:

**Enantioselective enzyme-catalyzed aziridination enabled by active-site
evolution of a cytochrome P450**

Christopher C. Farwell[†], Ruijie K. Zhang[†], John A. McIntosh, Todd K. Hyster, Frances H.

Arnold*

Division of Chemistry and Chemical Engineering, California Institute of Technology, 1200 E.

California Blvd, Pasadena, CA 91125, United States

*Correspondence addressed to frances@cheme.caltech.edu

Experimental Procedures

General. Unless otherwise noted, all chemicals and reagents were obtained from commercial suppliers (Sigma-Aldrich, VWR, Alfa Aesar) and used without further purification. Silica gel chromatography purifications were carried out using AMD Silica Gel 60, 230-400 mesh. ^1H spectra were recorded on a Varian Inova 300 MHz or 500 MHz, or Bruker Prodigy 400 MHz instrument in CDCl_3 , and are referenced to the residual solvent peak. Synthetic reactions were monitored using thin layer chromatography (Merck 60 gel plates) using an UV-lamp for visualization.

Chromatography. Analytical high-performance liquid chromatography (HPLC) was carried out using an Agilent 1200 series, and a Kromasil 100 C18 column (4.6 x 50 mm, 5 μm). Semi-preparative HPLC was performed using an Agilent XDB-C18 (9.4 x 250 mm, 5 μm). Analytical chiral HPLC was conducted using a supercritical fluid chromatography (SFC) system with isopropanol and liquid CO_2 as the mobile phase. Chiral OB-H and AS-H columns were used to separate aziridine and amido-alcohol enantiomers (4.6 x 150 mm, 5 μm). Olefins were all commercially available; amido-alcohol^{S1} and aziridine^{S2} standards were prepared as reported. %*ee* was calculated by dividing the major peak area by the sum of the peak areas determined by SFC chromatography.

Cloning and site-directed mutagenesis. pET22b(+) was used as a cloning and expression vector for all enzymes described in this study. Site-directed mutagenesis was performed using a modified QuikChangeTM mutagenesis protocol. The PCR products were gel purified, digested with DpnI, repaired using Gibson MixTM, and directly transformed into *E. coli* strain BL21(DE3).

Determination of P450 concentration. Concentration of P450/P411 enzymes in whole cell experiments was determined from ferrous carbon monoxide binding difference spectra using previously reported extinction coefficients for cysteine-ligated ($\epsilon = 91,000 \text{ M}^{-1} \text{ cm}^{-1}$) and serine-ligated enzymes ($\epsilon = 103,000 \text{ M}^{-1} \text{ cm}^{-1}$).^{S3} When purified enzymes were used, concentration of P450/P411 enzymes was accomplished by quantifying the amount of free hemin present in purified protein using the pyridine/hemochrome assay.^{S4}

Protein expression and purification. Enzymes used in purified protein experiments were expressed in *E. coli* strain BL21(DE3) transformed with plasmid encoding P450 or P411 variants. Expression and purification were performed as described except that the shake rate was lowered to 130 RPM during expression.^{S5} Following expression, cells were pelleted and frozen at -20 °C. For purification, frozen cells were resuspended in buffer A (20 mM tris, 20 mM imidazole, 100 mM NaCl, pH 7.5, 4 mL/g of cell wet weight), loaded with 300 µg/ml hemin, and disrupted by sonication (2 x 1 min, output control 5, 50% duty cycle; Sonicator 3000, Misonix, Inc.). To pellet insoluble material, lysates were centrifuged (20,000 x g for 0.5 h at 4 °C). Proteins were expressed in a construct containing a 6x-His tag and were consequently purified using a nickel NTA column (1 mL HisTrap HP, GE Healthcare, Piscataway, NJ) using an AKTExpress purifier FPLC system (GE healthcare). P450 or P411 enzymes were then eluted on a linear gradient from 0% buffer B (20 mM tris, 300 mM imidazole, 100 mM NaCl, pH 7.5) to 100 % buffer B over 10 column volumes (P450/P411 enzymes elute at around 80 mM imidazole). Fractions containing P450 or P411 enzymes were pooled, concentrated, and subjected to three exchanges of phosphate buffer (0.1 M potassium phosphate (KPi), pH 8.0) to remove excess salt and

imidazole. Concentrated proteins were aliquoted, flash-frozen on powdered dry ice, and stored at -20 °C until later use.

Reaction screening in 96-well plate format. Site-saturation mutagenesis libraries were generated by employing the “22c-trick” method.^{S6} *E. coli* libraries were generated and cultured in 300 µL of LB with 0.1 mg mL⁻¹ ampicillin and stored as glycerol stocks at -80 °C in 96-well plates. 50 µL of the pre-culture was transferred to a 1000 µL of Hyperbroth using a multichannel pipette. The cultures were incubated at 37 °C, 220 rpm, 80% humidity for 3 hours. The plates were cooled on ice for 15 minutes before expression was induced (0.5 mM IPTG, 1mM 5-aminolevulinic acid, final concentrations). Expression was conducted at 20 °C, 120 rpm, 20 h. The cells were pelleted (3000 x g, 5 min) and re-suspended in 40 µL/well GOX solution (14,000 U/ml catalase (Sigma 02071) and 1000 U/ml glucose oxidase (Sigma G7141)). The 96-well plate was transferred to an anaerobic chamber. In the anaerobic chamber, 300 µL per well argon sparged reaction buffer (4 : 1, M9-N : 250 mM glucose in M9-N) was added followed by 4-methylstyrene (300 mM, 10 µL/well) and tosyl azide (100 mM, 10 µL/well). The plate was sealed with aluminum sealing tape, removed from the anaerobic chamber, and shaken at 40 rpm. After 16 hours, the seal was removed and 400 µL of acetonitrile was added to each well. The contents of each well were mixed by pipetting up and down using a multichannel pipette. Then the plate was centrifuged (4000 x g, 5 minutes) and 500 µL of the supernatant was transferred to a shallow-well plate for analysis by HPLC.

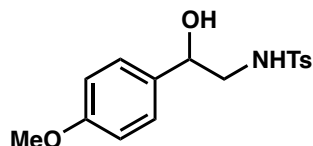
Typical procedure for small-scale aziridination bioconversions under anaerobic conditions using whole cells and purified enzymes. *E. coli* BL21(DE3) cells containing P450 or P411 enzymes were grown from glycerol stock overnight in 5 ml Luria broth with 0.1 mg mL⁻¹ ampicillin (37 °C, 250 rpm). The preculture was used to inoculate 45 mL of Hyperbroth medium (prepared from AthenaES© powder, 0.1 mg mL⁻¹ ampicillin) in a 125 mL Erlenmeyer flask; this culture was incubated at 37 °C, 220 rpm for 2 h and 30 min. After, the cultures were cooled on ice and induced with 0.5 mM IPTG and 1 mM 5-aminolevulinic acid (final concentration). Expression was conducted at room temperature, 120 rpm, 20 h. The cultures were then harvested and resuspended to OD₆₀₀ = 30 in M9-N. Aliquots of the cell suspension (4 mL) were used to determine the P450 or P411 expression level after lysis.

E. coli cells (OD₆₀₀ = 30) were made anaerobic by sparging with argon in a sealed 6 mL crimp vial for at least 30 minutes. To a 2 mL crimp vial was then added glucose (250 mM in M9-N, 40 µL) and the GOX solution described previously (20 µL). The headspace of the sealed 2 mL reaction vial was made anaerobic by flushing argon over the solution. Resuspended cells (320 µL), followed by olefin substrate (10 µL, 300 mM in DMSO), then tosyl azide (10 µL, 100 mM in DMSO) were added to 2 mL reaction vial via syringe under continuous flow of argon. Final concentrations of reagents were typically: 2.5 mM tosyl azide, 7.5 mM olefin, 25 mM glucose. The no enzyme control experiment was conducted using *E. coli* BL21 (DE3) cells containing empty pET22b(+) vector with the same reaction conditions as described above. Purified enzyme reactions were conducted as described previously, using 2.5 mM TsN₃ and 7.5 mM olefin.^{S9} Sodium dithionite (5 mM) was used as reductant for reactions with hemin, myoglobin, cytochrome *c*, CYP119, and P450_{Rhf}. The reactions were quenched by adding acetonitrile (460 µL) and the resulting mixture was transferred to a microcentrifuge tube and

centrifuged at 14,000 rpm for 5 minutes. The solution (540 μ L) was transferred to an HPLC vial, charged with internal standard (60 μ L, 10 mM 1,3,5-trichlorobenzene in acetonitrile), and analyzed by HPLC.

Reactions for chiral HPLC analysis were performed on a 2 mL scale using the same concentration of reagents and a similar procedure as described above. Briefly, cells containing P450 or P411 enzymes were expressed and resuspended to an $OD_{600} = 30$ in M9-N, and then degassed by sparging with argon in a sealed 6 mL crimp vial for at least 30 minutes. To a 6 mL crimp vial was then added glucose (250 mM in M9-N, 200 μ L) and the GOX mixture described previously (100 μ L). The headspace of the sealed 2 mL reaction vial was made anaerobic by flushing argon over the solution. Resuspended cells (1600 μ L), followed by olefin substrate (50 μ L, 300 mM in DMSO), then tosyl azide (50 μ L, 100 mM in DMSO) were added to 6 mL reaction vial via syringe under continuous flow of argon. Reactions were quenched with 2 mL acetonitrile, extracted with ethyl acetate, dried and resuspended in acetone (200 μ L), and purified by C18 semi-preparative HPLC. The purified material was dried, resuspended in acetonitrile, and analyzed by SFC for enantioselectivity.

Synthesis of substrates and standards. All olefins presented in main text Table 3 were obtained from commercial sources (Sigma Aldrich).

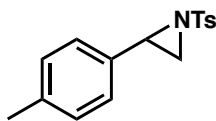


***N*-(2-hydroxy-2-(4-methoxyphenyl)ethyl)-4-methylbenzenesulfonamide (2).** Synthesized as previously reported.^{S1}

¹H NMR (400 MHz, CDCl₃): δ 7.72 (d, 2H, *J* = 8.1 Hz), 7.29 (d, 2H, *J* = 8.3 Hz), 7.19 (d, 2H, *J* = 8.6 Hz), 6.84 (d, 2H, 8.6 Hz), 5.06 (dd, 1H, *J* = 8.1, 4.6 Hz), 4.73 (dd, 1H, *J* = 8.7, 3.7 Hz), 3.78 (s, 3H), 3.20 (ddd, 1H, *J* = 13.3, 8.1, 3.7 Hz), 3.01 (ddd, 1H, *J* = 13.2, 8.6, 4.6 Hz), 2.42 (s, 3H)

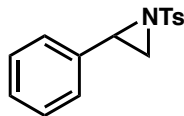
¹³C NMR (101 MHz, CDCl₃): δ 159.66, 143.69, 136.86, 133.00, 129.90, 127.26, 127.21, 114.16, 72.50, 55.44, 50.30, 21.66

HRMS (FAB⁺): calculated for C₁₆H₁₈NO₄S ([M+H]⁺): 320.0956; found: 320.0950



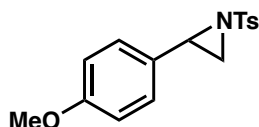
***N*-(*p*-Tolylsulfonyl)-2-(*p*-methylphenyl)aziridine (4).** Synthesized as previously reported^{S2} with spectral data in agreement with literature reported data.^{S10}

¹H NMR (300 MHz, CDCl₃): δ 7.86 (d, 2H, *J* = 8.3 Hz), 7.32 (d, 2H, *J* = 8.3 Hz), 7.10 (s, 4H), 3.74 (dd, 1H, *J* = 7.2, 4.5 Hz), 2.97 (d, 1H, *J* = 7.2 Hz), 2.43 (s, 3H), 2.38 (d, 1H, *J* = 4.5 Hz), 2.31 (s, 3H).



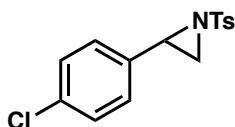
***N*-(*p*-Tolylsulfonyl)-2-phenylaziridine (6).** Synthesized as previously reported^{S2} with spectral data in agreement with literature reported data.^{S10}

$^1\text{H NMR}$ (300 MHz, CDCl_3): δ 7.87 (d, 2H, $J = 8.3$ Hz), 7.19-7.36 (m, 7H), 3.77 (dd, 1H, $J = 7.2, 4.5$ Hz), 2.98 (d, 1H, $J = 7.2$ Hz), 2.43 (s, 3H), 2.39 (d, 1H, $J = 4.5$ Hz)



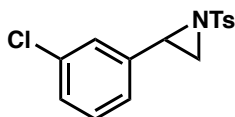
***N*-(*p*-Tolylsulfonyl)-2-(*p*-methoxyphenyl)aziridine (S1).** Synthesized as previously reported^{S2} with spectral data in agreement with literature reported data.^{S10}

$^1\text{H NMR}$ (500 MHz, CDCl_3): δ 7.87 (d, 2H, $J = 8.3$ Hz), 7.34 (d, 2H, $J = 8.5$ Hz), 7.14 (d, $J = 8.7$ Hz, 2H), 6.83 (d, $J = 8.7$, 2H), 3.78 (s, 3H), 3.75 (dd, 1H, $J = 7.2, 4.5$ Hz), 2.97 (d, 1H, $J = 7.2$ Hz), 2.44 (s, 3H), 2.39 (d, 1H, $J = 4.5$ Hz)



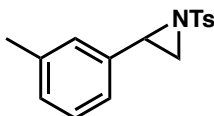
***N*-(*p*-Tolylsulfonyl)-2-(*p*-chlorophenyl)aziridine (S2).** Synthesized as previously reported^{S2} with spectral data in agreement with literature reported data.^{S10}

$^1\text{H NMR}$ (300 MHz, CDCl_3): δ 7.86 (d, 2H, $J = 8.3$ Hz), 7.34 (d, 2H, $J = 7.9$ Hz), 7.26 (d, 2H, $J = 8.5$ Hz), 7.15 (d, 2H, $J = 8.5$ Hz), 3.73 (dd, 1H, $J = 7.2, 4.4$ Hz), 2.98 (d, 1H, $J = 7.2$ Hz), 2.44 (s, 3H), 2.34 (d, 1H, $J = 4.4$ Hz)



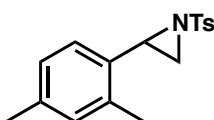
***N*-(*p*-Tolylsulfonyl)-2-(*m*-chlorophenyl)aziridine (S3).** Synthesized as previously reported^{S2} with spectral data in agreement with literature reported data.^{S11}

$^1\text{H NMR}$ (400 MHz, CDCl_3): δ 7.87 (d, 2H, $J = 8.3$ Hz), 7.35 (d, 2H, $J = 7.7$ Hz), 7.19 – 7.26 (m, 3H), 7.12 (dt, 1H, $J = 6.8, 1.8$ Hz), 3.73 (dd, 1H, $J = 7.2, 4.3$ Hz), 2.97 (d, 1H, $J = 7.2$ Hz), 2.44 (s, 3H), 2.35 (d, 1H, $J = 4.4$ Hz)



***N*-(*p*-Tolylsulfonyl)-2-(*m*-methylphenyl)aziridine (S4).** Synthesized as previously reported^{S2} with spectral data in agreement with literature reported values.^{S12}

¹H NMR (400 MHz, CDCl₃): δ 7.87 (d, 2H, *J* = 8.3 Hz), 7.33 (d, 2H, *J* = 8.6 Hz), 7.01 – 7.20 (m, 4H), 3.74 (dd, 1H, *J* = 7.2, 4.5 Hz), 2.96 (d, 1H, *J* = 7.2 Hz), 2.43 (s, 3H), 2.38 (d, 1H, *J* = 4.5 Hz), 2.30 (s, 3H)

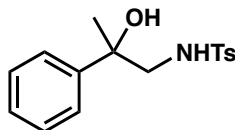


***N*-(*p*-Tolylsulfonyl)-2-(2,4-dimethylphenyl)aziridine (S5).** Synthesized as previously reported.^{S2}

¹H NMR (400 MHz, CDCl₃): δ 7.90 (d, 2H, *J* = 8.4 Hz), 7.34 (d, 2H, *J* = 8.5 Hz), 6.91 – 7.00 (m, 3H), 3.84 (dd, 1H, *J* = 7.2, 4.6 Hz), 2.97 (d, 1H, *J* = 7.2 Hz), 2.44 (s, 3H), 2.35 (s, 3H), 2.32 (d, 1H, *J* = 4.6 Hz), 2.28 (s, 3H)

¹³C NMR (101 MHz, CDCl₃): δ 144.72, 137.95, 136.72, 135.15, 130.89, 130.32, 129.84, 128.11, 126.82, 125.98, 39.61, 35.07, 21.75, 21.11, 19.08

HRMS (FAB⁺): calculated for C₁₇H₂₀NO₂S ([M+H]⁺): 302.1215; found: 302.1210

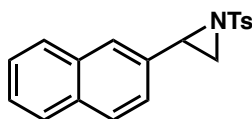


***N*-(2-hydroxy-2-phenylpropyl)-4-methylbenzenesulfonamide (S6).** Synthesized as previously reported.^{S1}

¹H NMR (400 MHz, CDCl₃): δ 7.67 (d, 2H, *J* = 8.3 Hz), 7.24 – 7.38 (m, 7H), 4.59 (s, 1H), 3.22 (dd, 1H, *J* = 12.8, 8.5 Hz), 3.12 (dd, 1H, *J* = 12.8, 4.8 Hz), 2.42 (s, 3H), 1.56 (s, 3H)

¹³C NMR (101 MHz, CDCl₃): δ 144.87, 143.73, 136.73, 129.93, 128.75, 127.60, 127.19, 124.93, 73.81, 53.99, 27.62, 21.68

HRMS (FAB⁺): calculated for C₁₆H₂₀NO₃S ([M+H]⁺): 306.1164; found: 306.1160



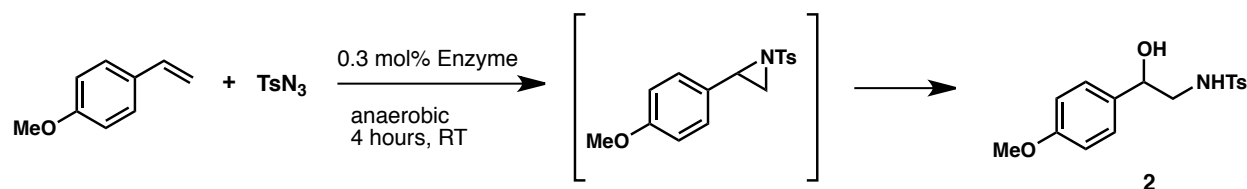
***N*-(*p*-Tolylsulfonyl)-2-(2-naphthyl)aziridine (S7).** Synthesized as previously reported^{S2} with spectral data in agreement with literature reported values.^{S10}

¹H NMR (400 MHz, CDCl₃): δ 7.90 (d, 2H, *J* = 8.3 Hz), 7.75 – 7.81 (m, 3H), 7.73 (s, 1H), 7.45 – 7.49 (m, 2H), 7.33 (d, 2H, *J* = 8.3 Hz), 7.25 – 7.30 (m, 1H), 3.93 (dd, 1H, *J* = 7.2, 4.4 Hz), 3.07 (d, 1H, *J* = 7.2 Hz), 2.50 (d, 1H, *J* = 4.5 Hz), 2.42 (s, 3H)

Table S1. Mutations present in P450_{BM3} variants used in this work.

Enzyme	Mutations relative to wild-type P450_{BM3}
P450_{BM3}	none
P450_{BM3}-T268A	T268A
P411_{BM3}	C400S
P411_{BM3}-T268A	T268A, C400S
P450_{BM3}-CIS	V78A, F87V, P142S, T175I, A184V, S226R, H236Q, E252G, T268A, A290V, L353V, I366V, E442K
P450_{BM3}-CIS-T438S	P450 _{BM3} -CIS T438S
P411_{BM3}-CIS-T438S	P450 _{BM3} -CIS C400S T438S
P-I263F	P411 _{BM3} -CIS T438S I263F
P-I263F-A328V	P411 _{BM3} -CIS T438S I263F A328V
P-I263F-A328V-L437V	P411 _{BM3} -CIS T438S I263F A328V L437V
P411_{BM3}-CIS A268T T438S	P411 _{BM3} -CIS A268T T438S
P411_{BM3} H2-A-10	P411 _{BM3} -CIS L75A L181A
P411_{BM3} H2-5-F10	P411 _{BM3} -CIS L75A I263A L437A
P411_{BM3} H2-4-D4	P411 _{BM3} -CIS L75A M177A L181A L437A

Table S2. Panel of P450_{BM3} purified enzymes tested for aziridination reactivity with 4-methoxystyrene **1**.



Entry	Enzyme	TTN 2
1	P411 _{BM3} -CIS T438S	15
2	P450 _{BM3} -CIS T438S	< 1
3	P450 _{BM3} -CIS T438S C400H	3
4	P450 _{BM3} -CIS T438S C400D	4
5	P450 _{BM3} -CIS T438S C400M	4
6	P411 _{BM3} -CIS A268T T438S	< 1
7	P411 _{BM3} -H2-5-F10	8
8	P411 _{BM3} -H2-A-10	4
9	P411 _{BM3} -H2-4-D4	5
10	P450 _{BM3}	< 1
11	P411 _{BM3}	3
12	P450 _{BM3} -T268A	2
13	P411 _{BM3} -T268A	4
14	P411 _{BM3} -CIS T438S I263F	150
15	P411 _{BM3} -CIS T438S I263F V87F	19
16	P411 _{BM3} -CIS T438S I263F A268T	< 1

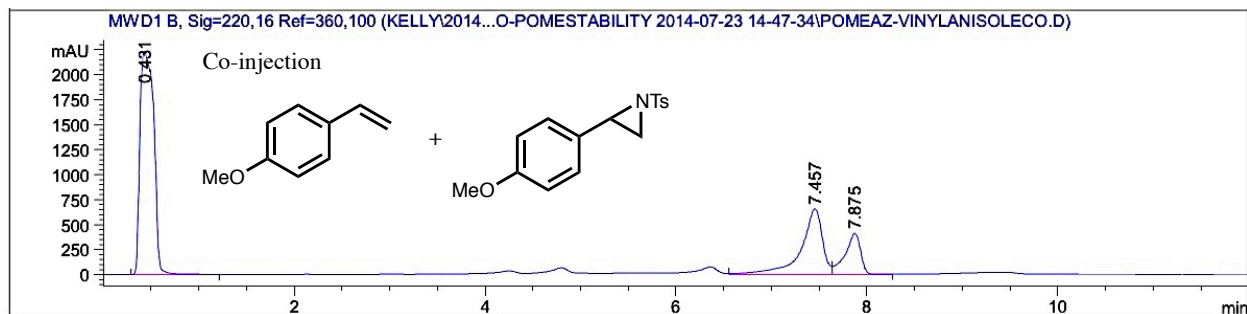
Table S3. Heme and other heme-containing proteins tested for activity in the above reaction (Table S2) with 4-methoxystyrene. Myoglobin and cytochrome *c* were purchased as lyophilized powder from Sigma Aldrich. P450_{Rhf} mutants were expressed and purified as described in the methods section; P450_{CYP119} was expressed and purified as described previously.^{S14}

Entry	Catalyst	TTN 2
1	Hemin	< 1
2	Hemin + BSA	< 1
3	Myoglobin (horse heart)	< 1
4	Cytochrome <i>c</i> (bovine heart)	< 1
5	CYP119 C317S	7
6	CYP119 T213A C317H	< 1
7	P450 _{Rhf}	< 1
8	P450 _{Rhf} T275A	< 1

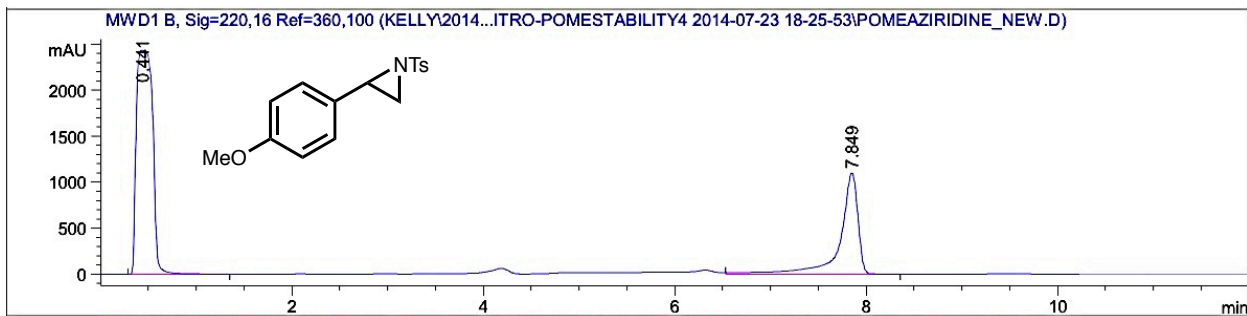
Figure S1. Demonstration of enzymatic synthesis and degradation of aziridine S1 in reaction conditions

A. HPLC chromatogram (220 nm) of controls.

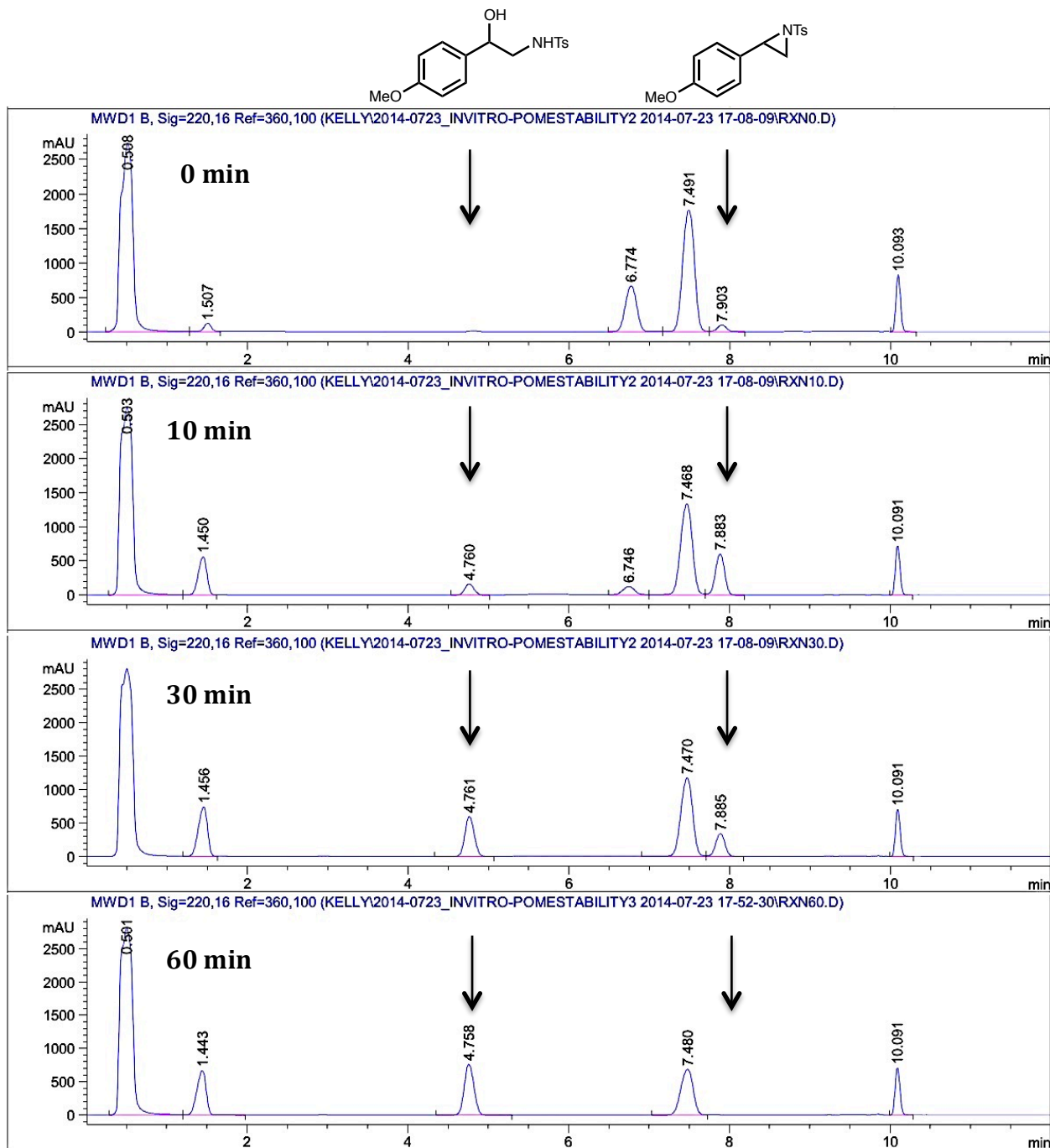
Co-injection of 4-methoxystyrene (Sigma Aldrich) and synthetic standard S1, confirmed by NMR.



Synthetic standard S1, confirmed by NMR



B. HPLC chromatograms (220 nm) of P411-enzymatic reaction with 4-methoxystyrene **1** and tosyl azide as substrates analyzed at different time points. Putative aziridine **S1** and amidoalcohol **2** are marked with arrows.



C. HPLC chromatograms (220 nm) of synthetic standard **S1**, synthesized as previously reported,^{S2} in reaction conditions *without* P411 catalyst at several time points. Putative aziridine **S1** and amido-alcohol **2** are marked with arrows.

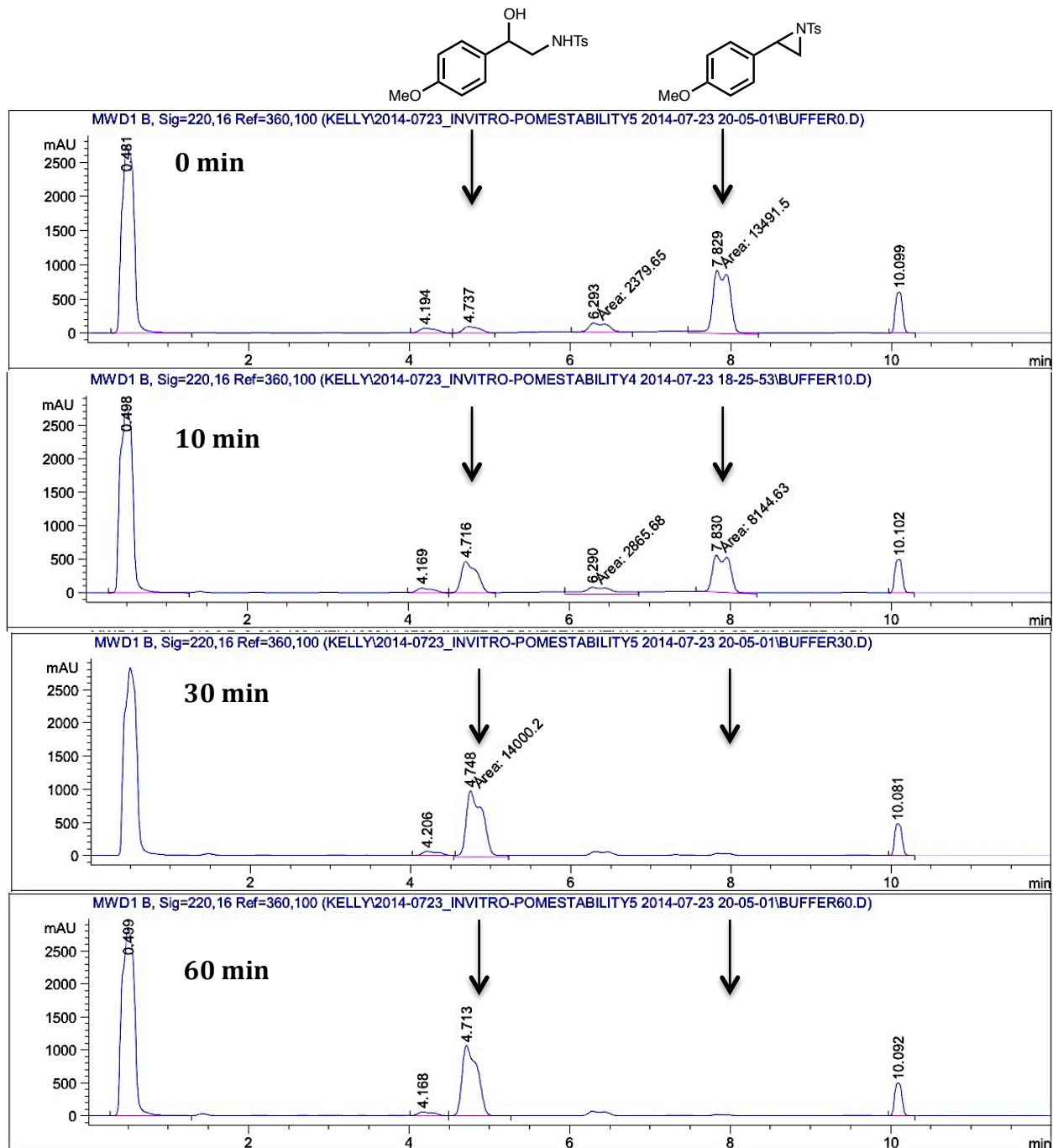
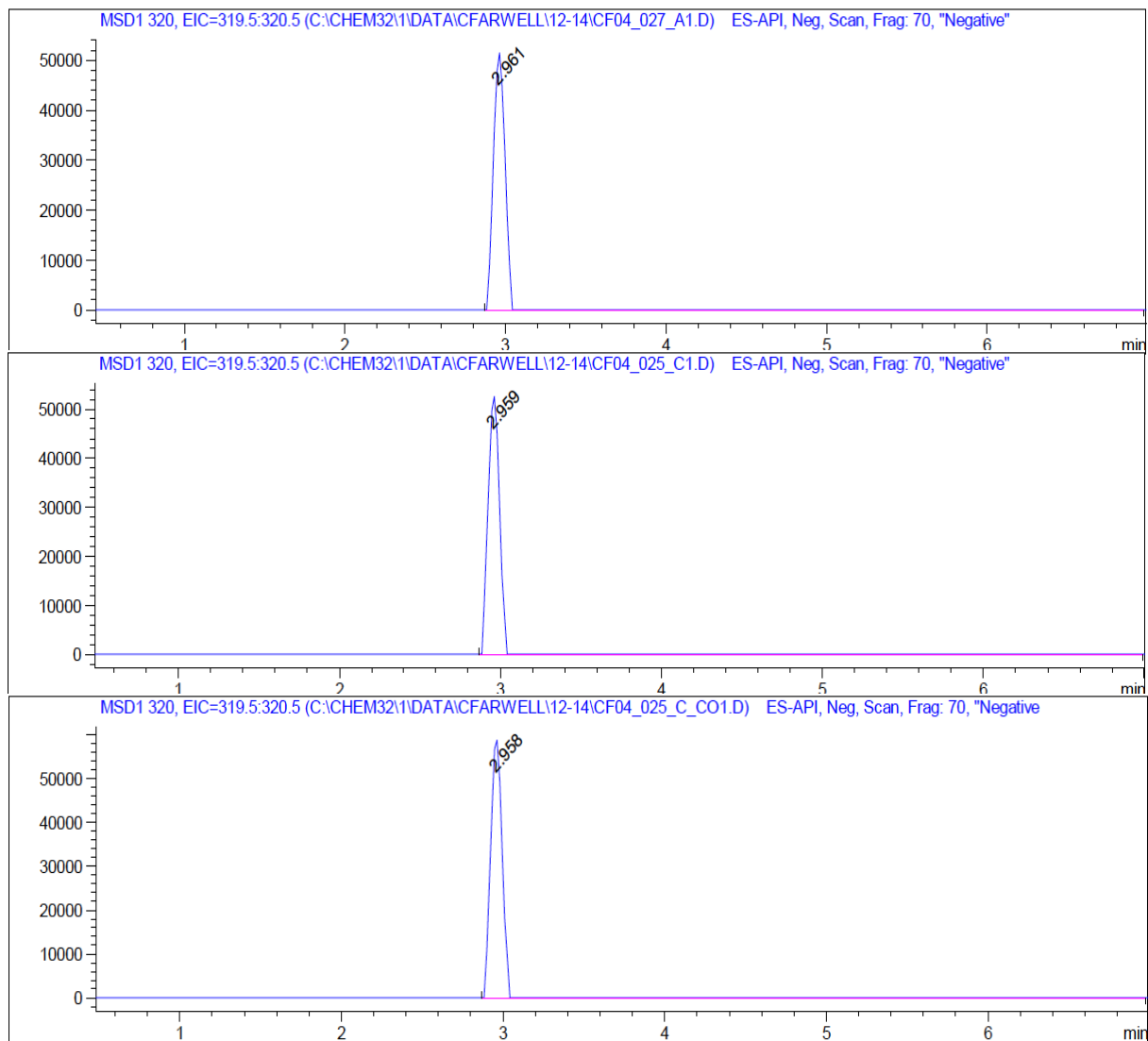


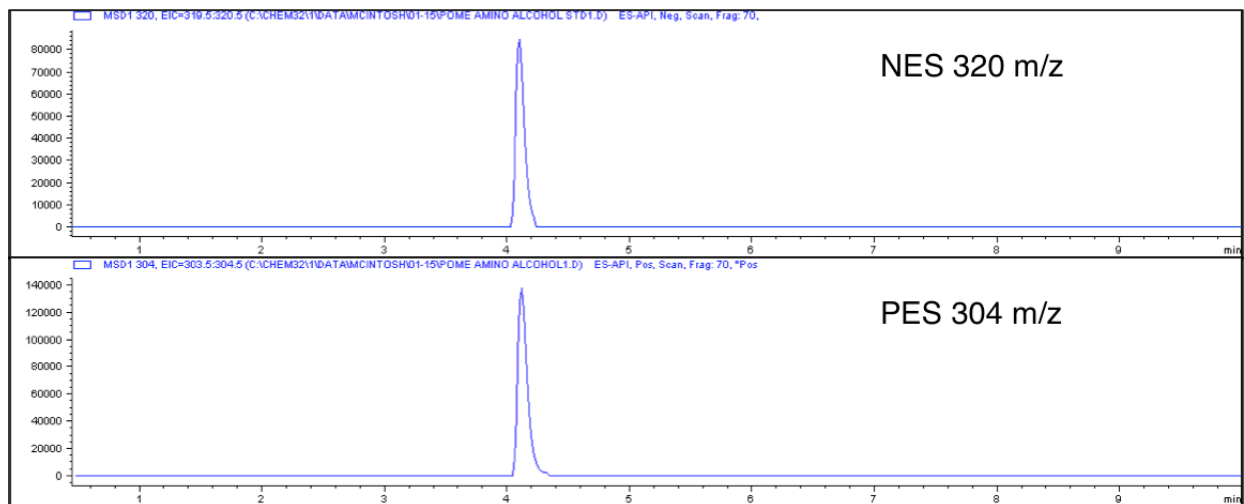
Figure S2. A. Demonstration of enzymatic production of 2.

Chromatogram traces are shown for the selected ion at 320 m/z in negative ionization mode. Top: synthetic standard of **2** prepared as stated above. Middle: enzymatically produced **2**. Bottom: mixture of enzyme reaction and synthetic **2**, showing coelution.



B. Detection of aziridine mass peak in pure sample of amido-alcohol 2.

Amido-alcohol **2** gives a mass peak of 304 m/z (mass corresponding to **S1**) when analyzed by LC-MS with positive electrospray (PES) ionization. This phenomenon is thought to occur via acid-catalyzed dehydration of the amido-alcohol in the MS system.



C. Demonstration of enzymatic production of 4.

Chromatogram traces are shown for the selected ion at 288 m/z in positive ionization mode. Top: synthetic standard of 5 prepared as stated above. Middle: enzymatically produced 4. The peak at retention time 3.33 is thought to be aziridine that degraded to the corresponding amido-alcohol as described in Figure S1 above. Bottom: mixture of enzyme produced and synthetic 4, showing coelution.

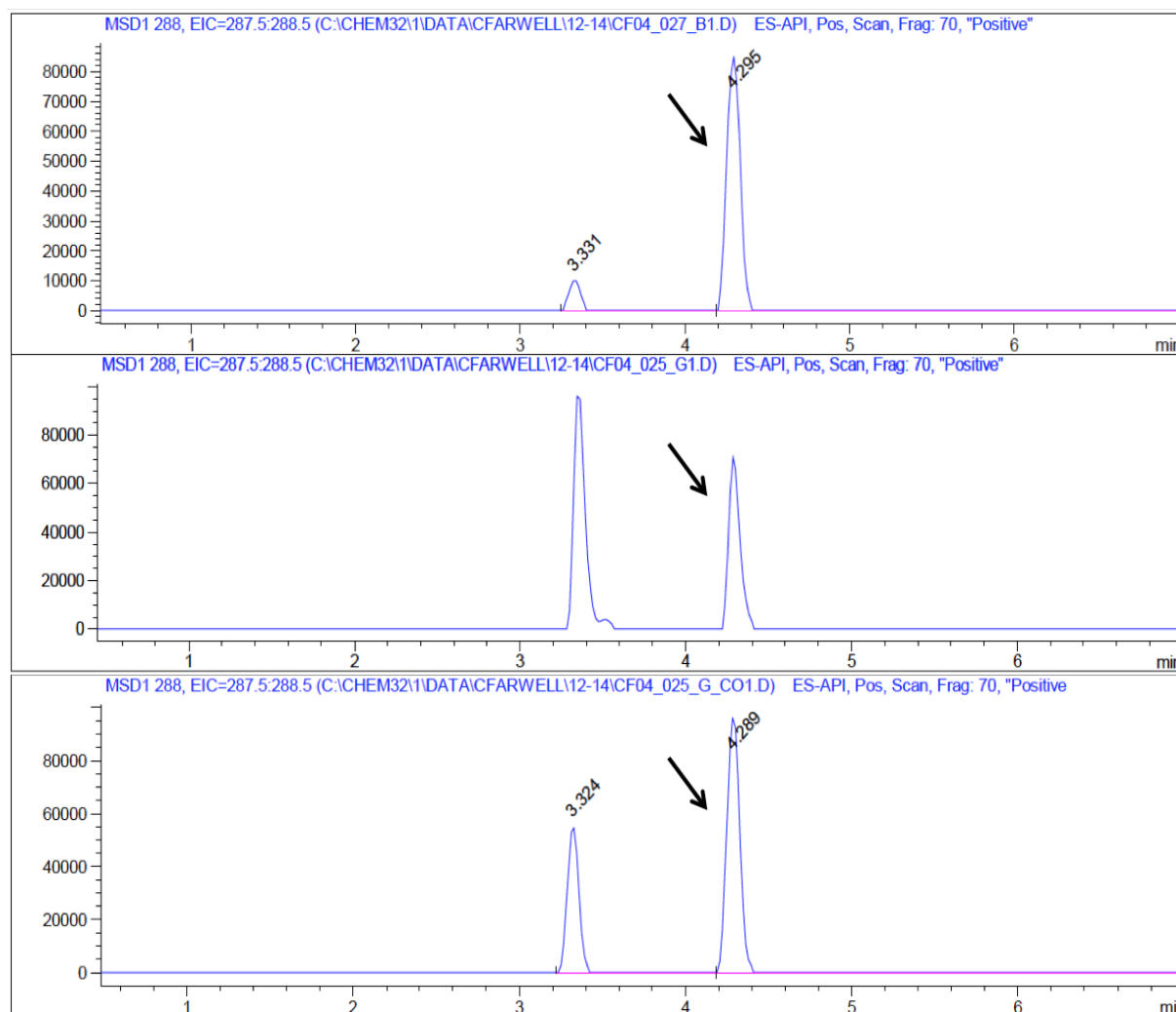
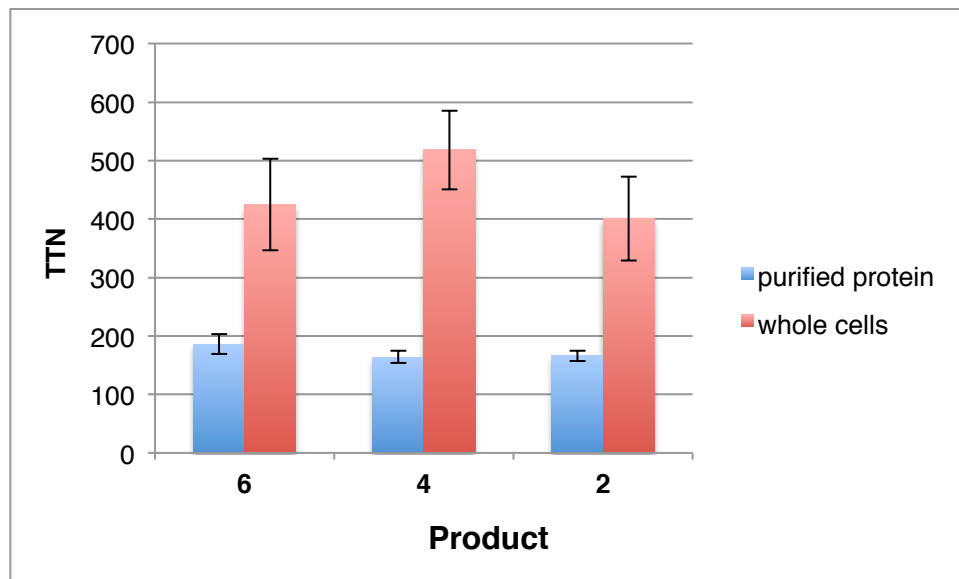


Figure S3. Comparison of P -I263F productivity *in vitro* (purified protein) and in whole cells.



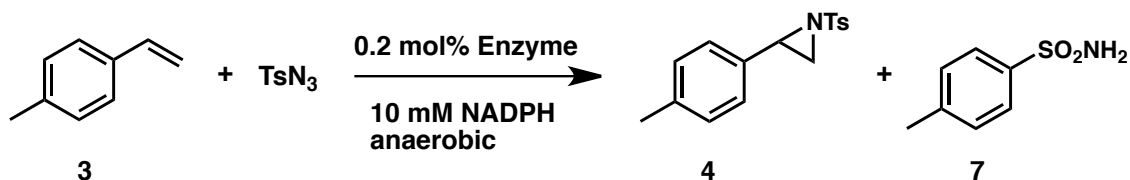
Determination of Initial Rates

All initial rate experiments were conducted in an anaerobic chamber. Initial rate measurements were accomplished using 0.2 mol% purified enzymes in 400 μL scale reactions. A sealed 6-mL vial charged with glucose (250 mM, 480 μL), NADPH (100 mM, 480 μL), and potassium phosphate buffer (0.1 M, pH = 8.0, 3240 μL) was sparged for at least 30 minutes with argon. After the degassing was complete, the reaction solution, 2-mL vials charged with GOX solution (20 μL), and purified protein (250 μM in potassium phosphate buffer), kept on ice, were brought into the anaerobic chamber. The reaction solution (350 μL) was added to each 2-mL vial and allowed to equilibrate in the anaerobic chamber for 30 minutes. Reaction vials were then placed on a shaker (40 rpm), charged with 10 μL purified protein (250 μM in potassium phosphate buffer) and 4-methyl styrene substrate (10 μL , 300 mM in DMSO) followed by tosyl azide (10 μL , 100 mM in DMSO). Reactions were set up in duplicate and products quantified at 1-2

minute intervals by quenching with acetonitrile (460 μL). The resulting mixture was removed from the anaerobic chamber, transferred to a microcentrifuge tube and centrifuged at 14,000 rpm for 5 minutes. The solution (540 μL) was transferred to an HPLC vial, charged with internal standard (60 μL , 10 mM 1,3,5-trichlorobenzene in acetonitrile), and analyzed by HPLC. The rates of aziridination and azide reduction for different enzyme variants are presented in Table S4. The rate of azide reduction was determined in the presence of olefin **3** (7.5 mM).

Table S4. Initial rates of aziridination and azide reduction for engineered enzymes

Initial rates determined as described above. Total turnover (TTN) values were determined using the same method as described for initial rates, with the exception that reactions were allowed to proceed for 4 hours in the anaerobic chamber.

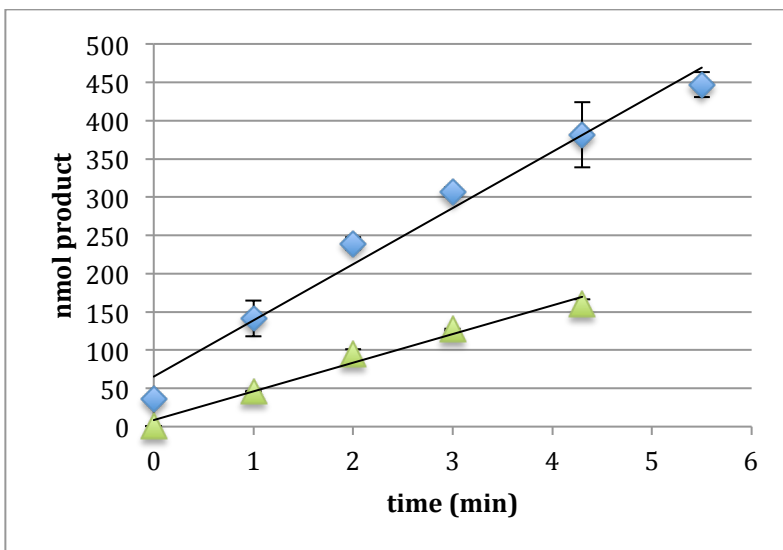


Enzyme	TOF 4 (min^{-1})	TOF 7 (min^{-1})	TOF 4/ TOF 7	TTN 4	TTN 7	TTN 4/ TTN 7
P-I263F	15	29	0.51	150	280	0.52
P-I263F-A328V	16	26	0.62	145	290	0.50
P-I263F-A328V-L437V	24	29	0.83	185	250	0.73

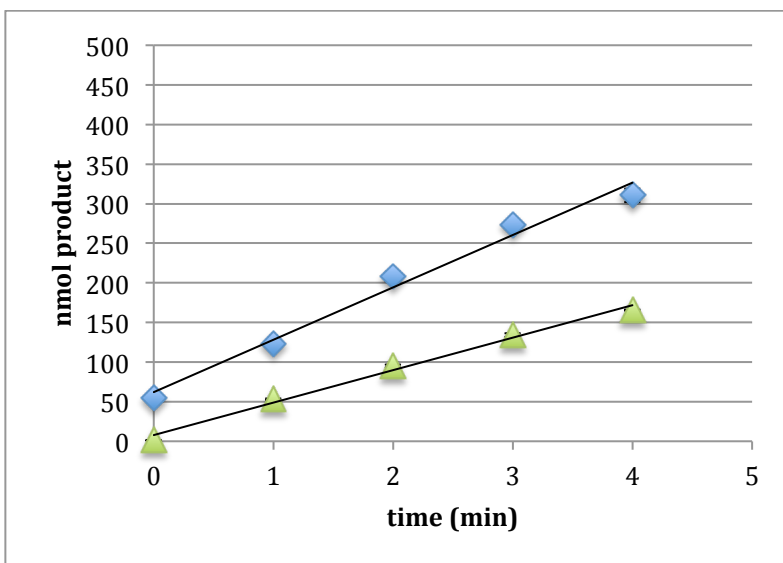
Figure S4. Data used to determine initial rates

Blue diamonds represent tosyl sulfonamide **7** and green triangles represent aziridine **4** for all plots.

A) P-I263F



B) P-I263F-A328V



C) P-I263F-A328V-L437V

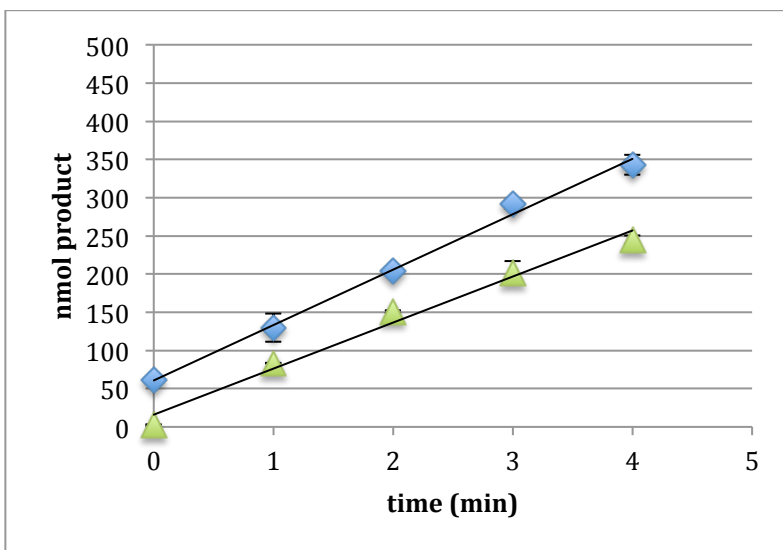


Figure S5. Activity and selectivity of P-I263F-A328V-L437V with increased substrate loading. Reactions were performed with whole *E. coli* cells expressing P-I263F-A328V-L437V as described in the general methods, except substrate loading was increased to final concentrations of 7.5 mM tosyl azide and 15 mM olefin. % *ee* determined by SFC analysis and calculated as $(S - R)/(S + R)$.

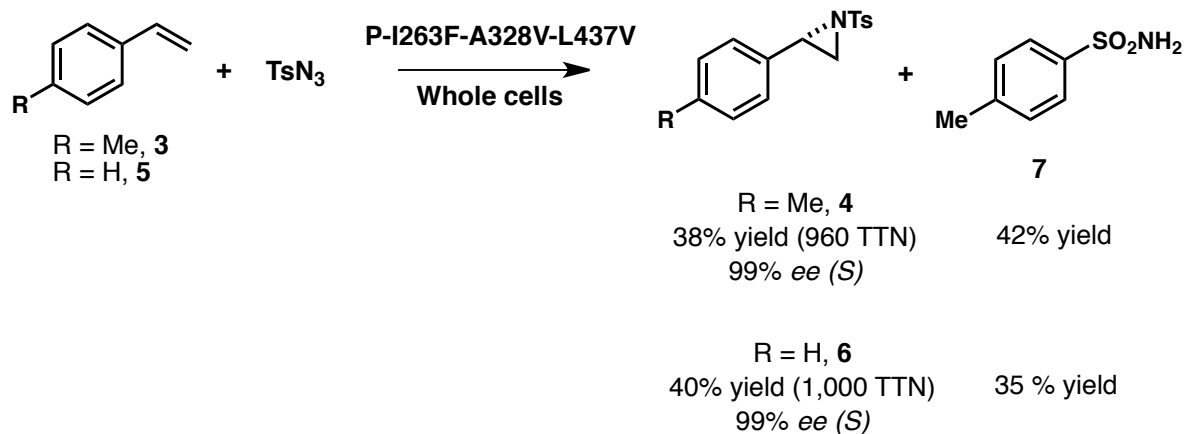
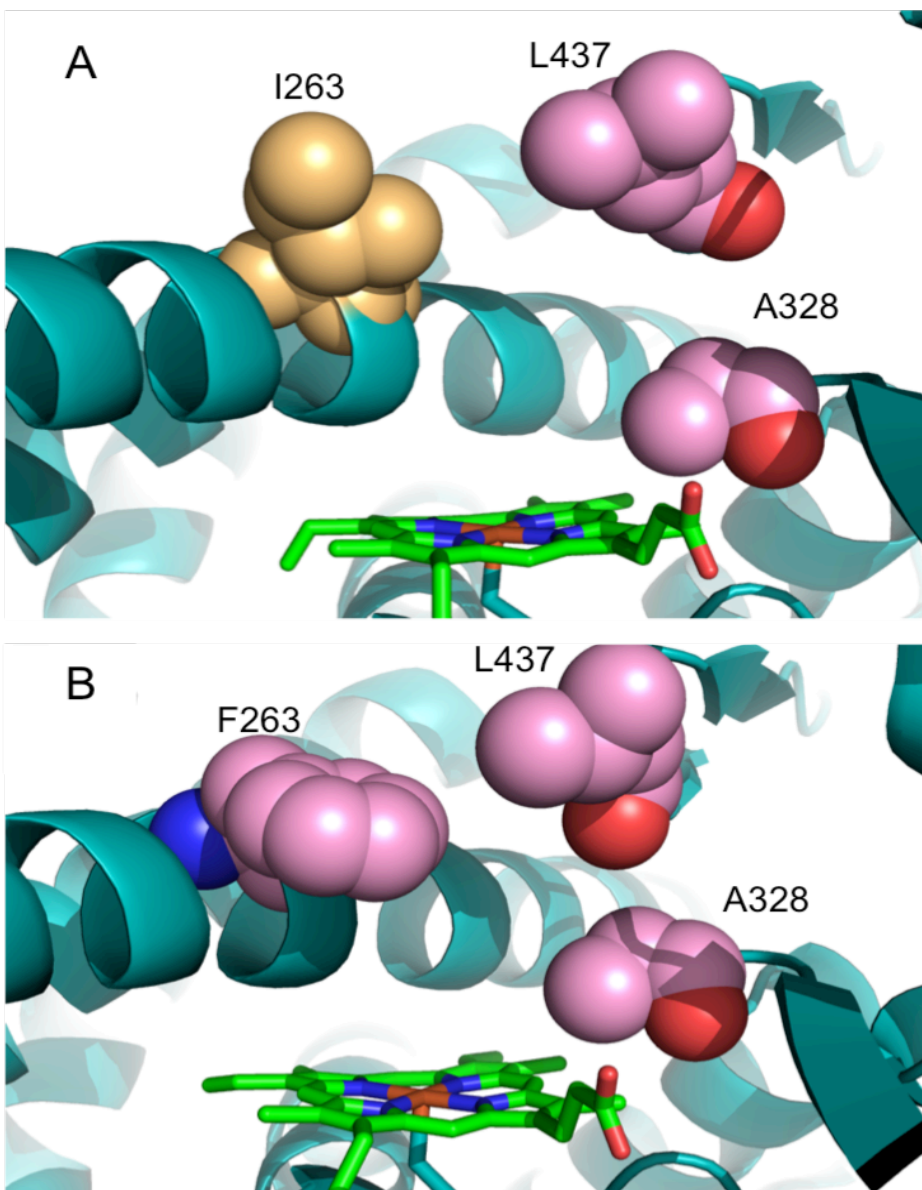


Figure S6. Comparison of active site residues in P411_{BM3}-CIS and P-I263F

A) P411_{BM3}-CIS structure (PDB ID: 4H23) with I263 shown as van Der Waals spheres in gold, L437 and A328 shown in pink. B) P-I263F structure (PDB ID: 4WG2) showing the active site and residues F263, A328 and L437 in pink.



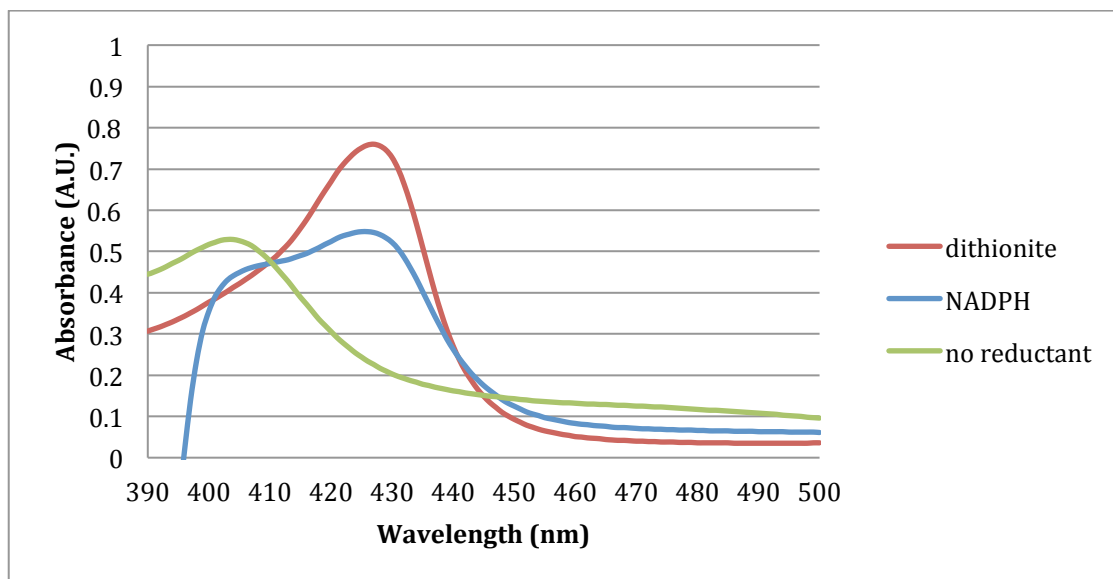
UV-Visible absorbance spectroscopy under anaerobic conditions.

A sealed 6-mL vial charged with potassium phosphate buffer (0.1 M, pH = 8.0, 4 mL) and a sealed 2-mL vial charged with NADPH (100 mM, 1 mL) were sparged for at least 20 minutes with argon. In parallel, purified full-length P-I263F (200 μ M, 25 μ L) or heme domain only P-I263F_{heme} (250 μ M, 20 μ L) was added to a semi-micro cuvette. The cuvette was sealed with a cap equipped with rubber septa and the headspace was purged with argon for at least 10 minutes. After degassing was complete, potassium phosphate buffer (880 μ L), followed by NADPH (100 mM, 100 μ L), were added to the anaerobic cuvette containing protein via syringe under a continuous stream of argon. UV-vis spectra of the protein sample was recorded until a stable ferrous state was reached, or for 20 minutes if no ferrous state was observed.

The negative control (no reductant) and positive control (dithionite-reduced protein) experiments were performed in a similar manner except degassed potassium phosphate buffer (100 μ L, negative control) or degassed dithionite solution (100 mM, 100 μ L, positive control) was added to the protein sample instead of NADPH.

Figure S7. UV-vis absorbance spectra of full-length P-I263F and P-I263F_{heme} proteins after addition of NADPH. Representative UV-vis absorbance spectra are shown for purified protein in the presence of no reductant (Fe^{III}, green), NADPH (blue), and dithionite (Fe^{II}, red). In the case of full-length P-I263F, the Fe^{II} (426 nm) Soret band is observed when either NADPH or dithionite is used as reductant. The shoulder at 404 nm observed in the NADPH spectrum is due to incomplete reduction of full-length P-I263F under the experimental conditions. For P-I263F_{heme}, only the Fe^{III} (404 nm) Soret band is observed when NADPH is used as the reductant.

A) P-I263F



B) P-I263F_{heme}

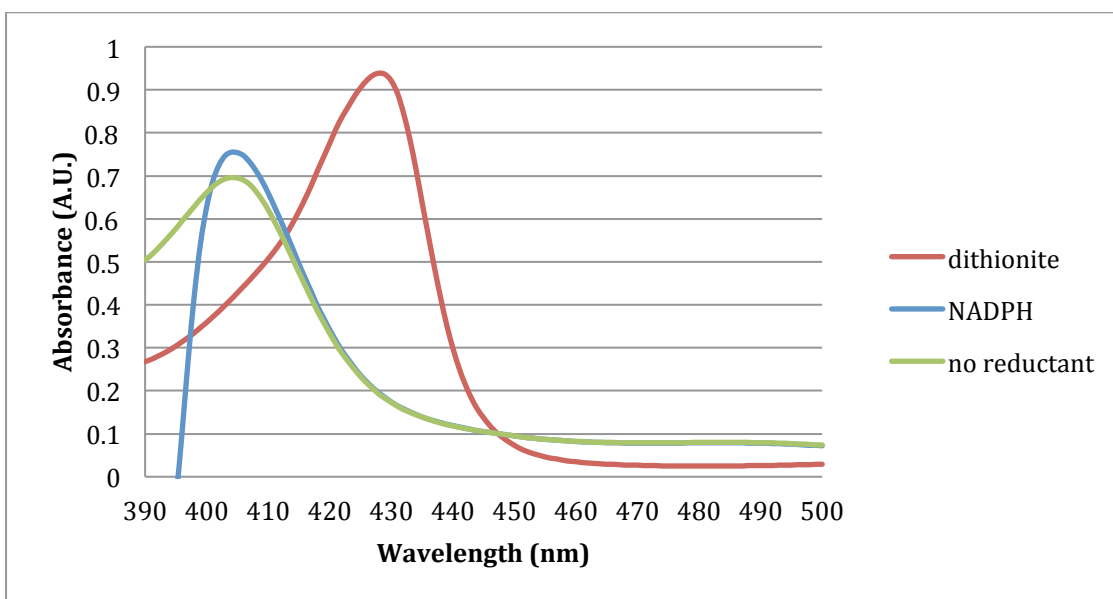


Figure S8. Demonstration of enzymatic production of 6.

Chromatogram traces are shown for the selected ion at 274 m/z in positive ionization mode. Top: synthetic standard of **6** prepared as stated above. Middle: enzymatically produced **6**. Bottom: mixture of enzyme reaction and synthetic **6**, showing coelution.

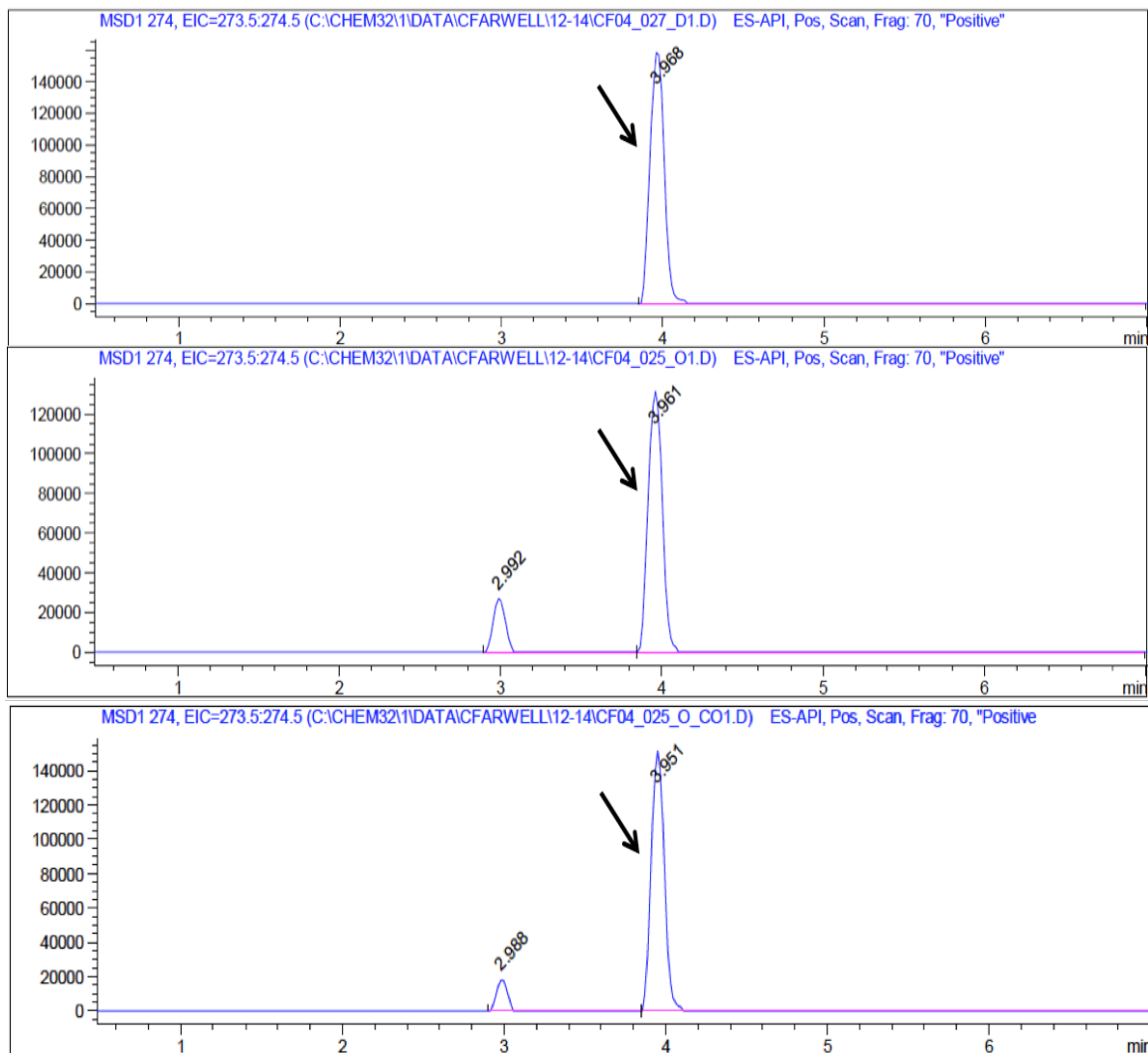


Figure S9. Demonstration of enzymatic production of S2.

Chromatogram traces are shown for the selected ion at 308 m/z in positive ionization mode. Top: synthetic standard of S2 prepared as stated above. Middle: enzymatically produced S2. Bottom: mixture of enzyme reaction and synthetic S2, showing coelution.

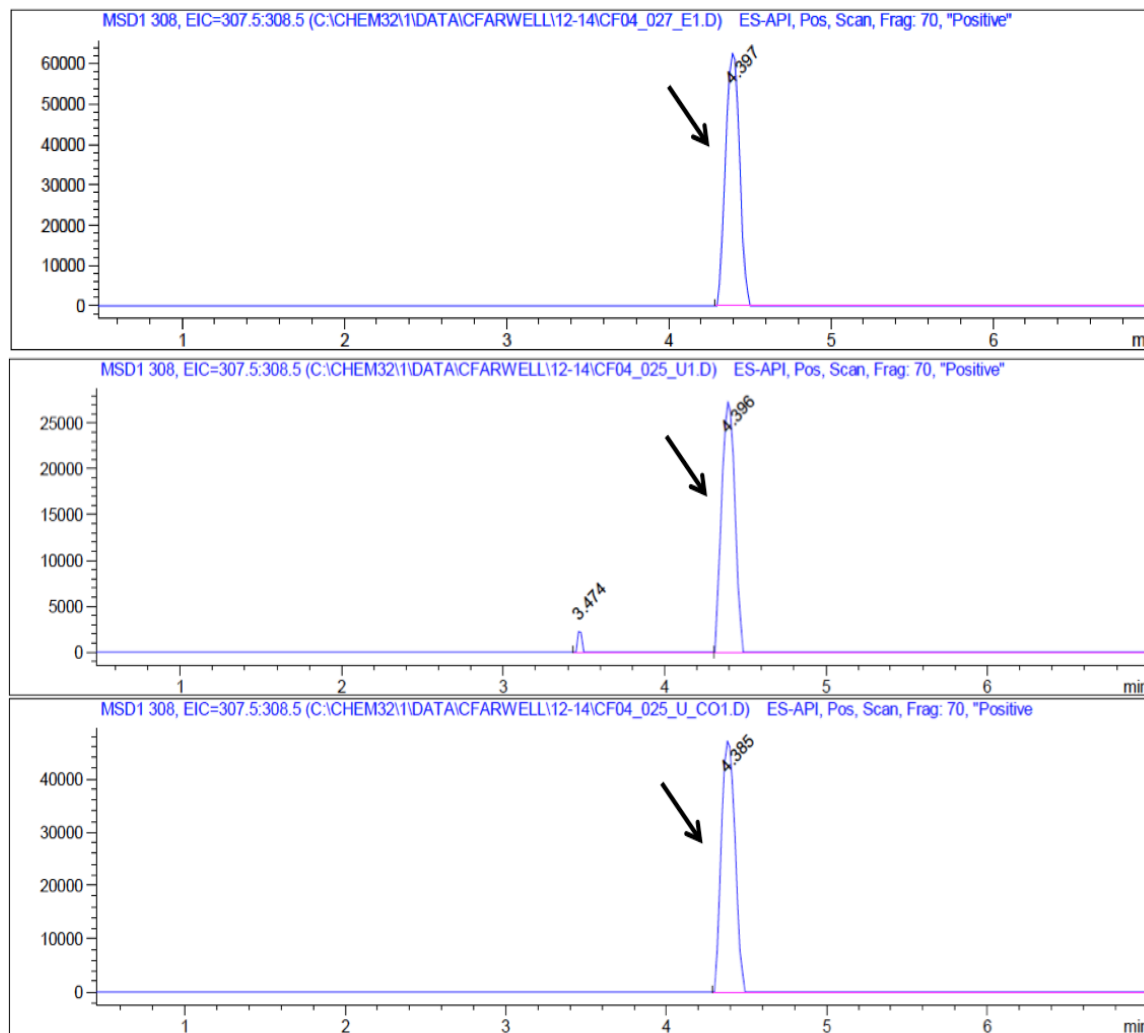


Figure S10. Demonstration of enzymatic production of S4.

Chromatogram traces are shown for the selected ion at 288 m/z in positive ionization mode. Top: synthetic standard of S4 prepared as stated above. Middle: enzymatically produced S4. Bottom: mixture of enzyme reaction and synthetic S4, showing coelution.

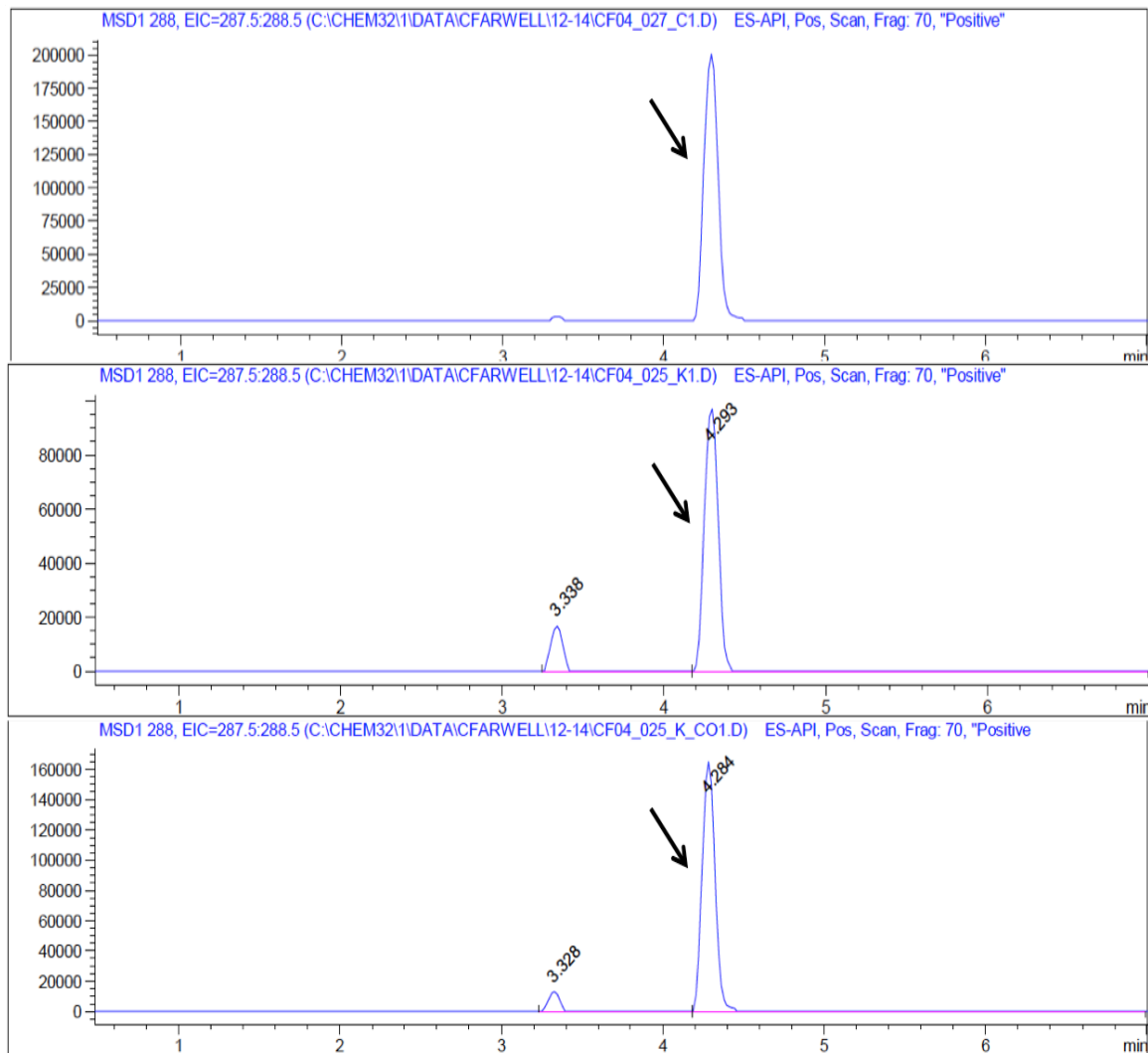


Figure S11. Demonstration of enzymatic production of S5.

Chromatogram traces are shown for the selected ion at 302 m/z in positive ionization mode. Top: synthetic standard of S5 prepared as stated above. Middle: enzymatically produced S5. Bottom: mixture of enzyme reaction and synthetic S5, showing coelution.

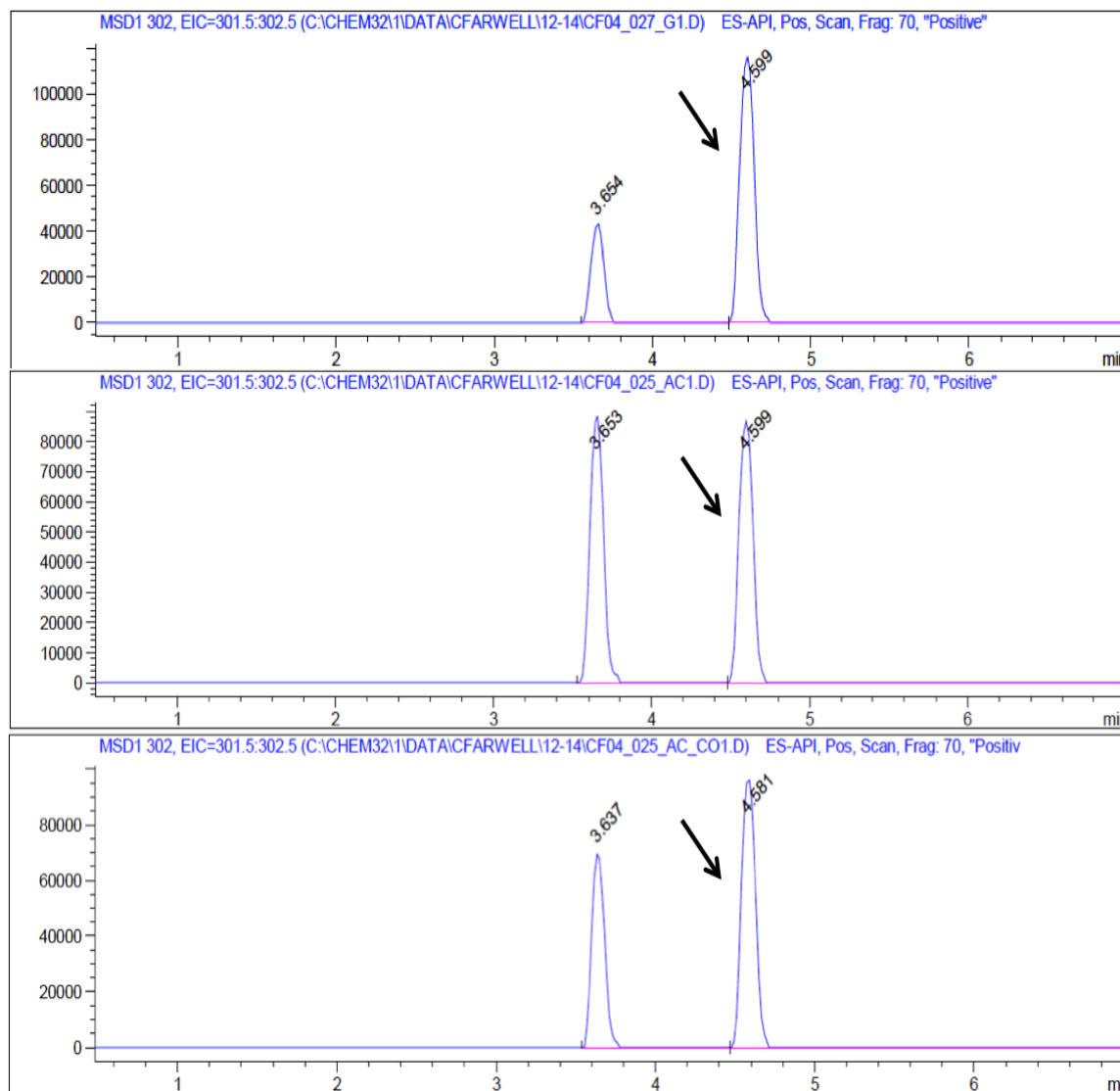


Figure S12. Demonstration of enzymatic production of S6

Chromatogram traces are shown for the selected ion at 304 m/z in negative ionization mode. Top: synthetic standard of S6 prepared as stated above. Middle: enzymatically produced S6. Bottom: mixture of enzyme reaction and synthetic S6, showing coelution.

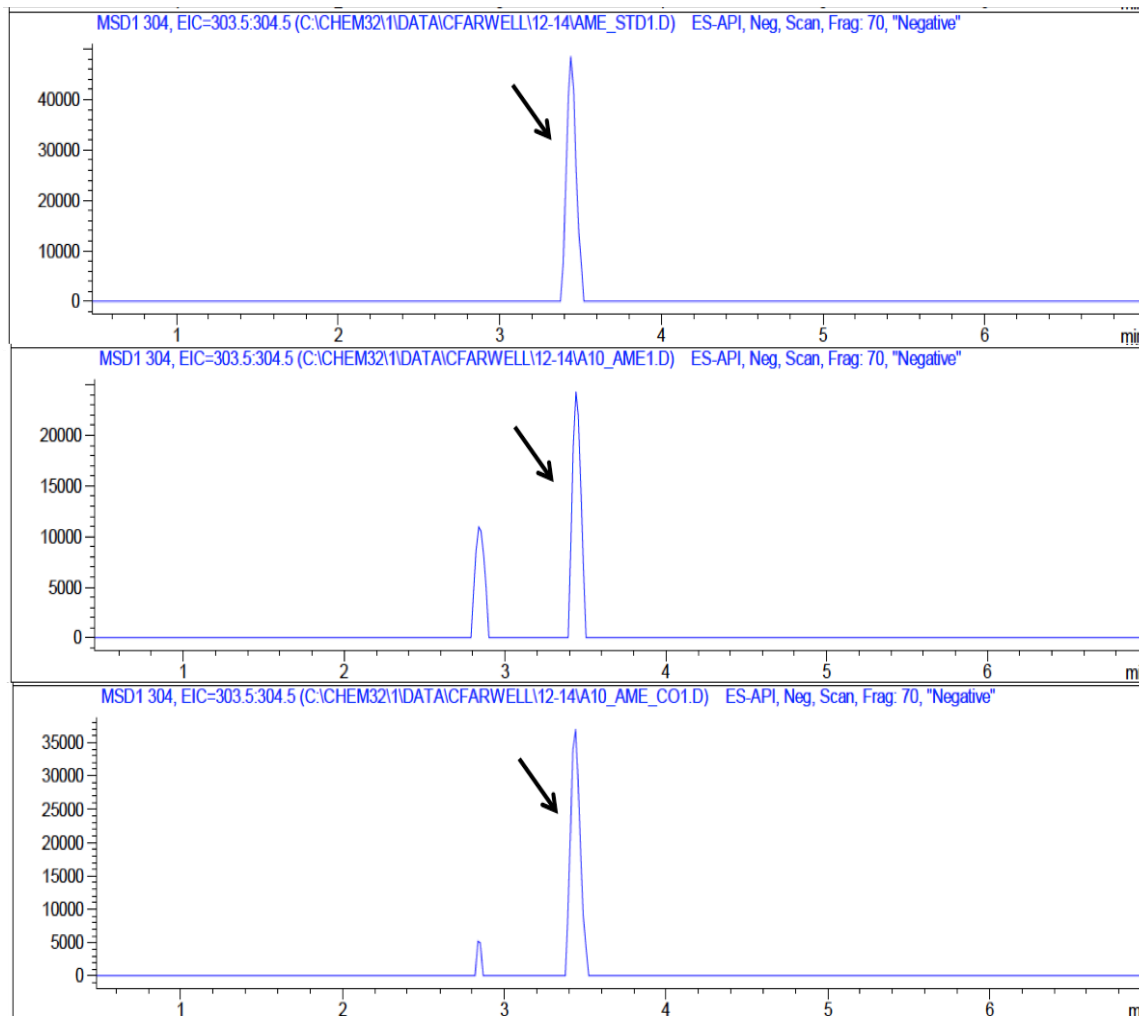
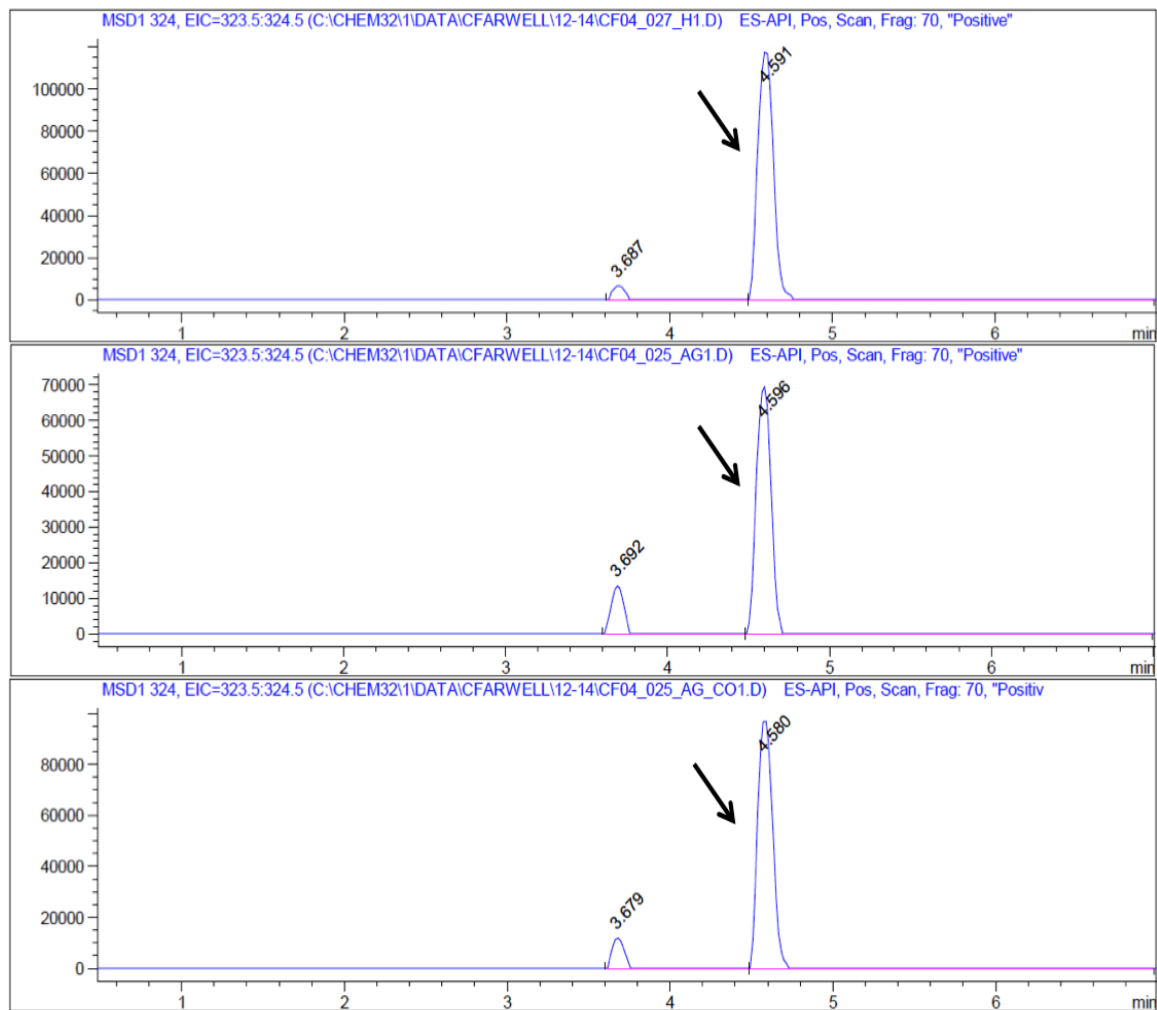
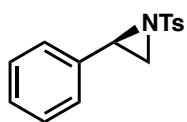


Figure S13. Demonstration of enzymatic production of S7.

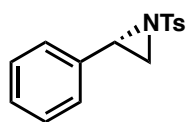
Chromatogram traces are shown for the selected ion at 324 m/z in positive ionization mode. Top: synthetic standard of S7 prepared as stated above. Middle: enzymatically produced S7. Bottom: mixture of enzyme reaction and synthetic S7, showing coelution.



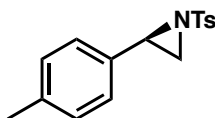
Assignment of absolute stereochemistry. Absolute stereochemistry of enzymatically produced aziridine **6** was assigned by chiral HPLC analysis and optical rotation. In particular, absolute stereochemistry of **6** was previously assigned by chiral HPLC using Chiracel OJ column (isopropanol/ n-hexane mobile phase), with (*S*)-**6** the earlier eluting enantiomer.^{S7} Analytically enantiopure **6** produced by P-I263F-A328V-L437V (whole cells) was subjected to the same chiral HPLC conditions and observed to be the earlier eluting enantiomer (Figure S14), leading to an assignment of (*S*)-**6**. Further support for this assignment came from measuring optical rotation. The optical rotation values for enantiomers of **6** have been previously reported: (*R*)-**6** [α_D^{24}] -80.25 (c =0.8, CHCl₃) and (*S*)-**6** [α_D^{20}] +26.7 (c =0.7, CHCl₃).^{S8} Optical rotation measurement of analytically enantiopure **6** produced by P-I263F-A328V-L437V gave [α_D^{25}] +80.2 (c =1.2, CHCl₃), revealing it to be (*S*)-**6**. Similarly, the optical rotation of P-I263F-A328V-L437V produced **4** (analytically enantiopure) was measured to be [α_D^{25}] +106.1 (c =0.45, CHCl₃). By analogy, the configuration of enzymatically preferred (+)-**4** is assigned as (*S*)-**4**.



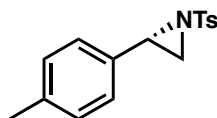
(-)-**6**



(+)-**6**



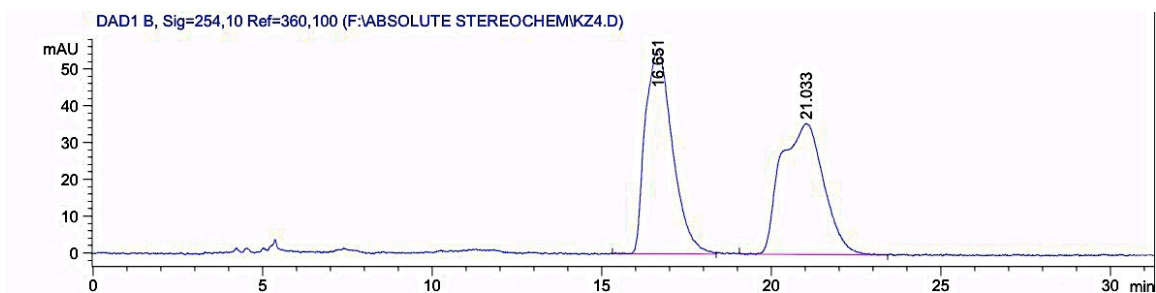
(-)-**4**



(+)-**4**

Figure S14. Assignment of absolute stereochemistry of enzymatically produced aziridine 6 by chiral HPLC (Chiracel OJ, 30% isopropanol : 70% n-hexane, 210 nm).

Racemic synthetic aziridine 6, $t_R = 16.7$ min and 21.0 min.



P-I263F-A328V-L437V produced aziridine 6, $t_R = 16.8$ min.

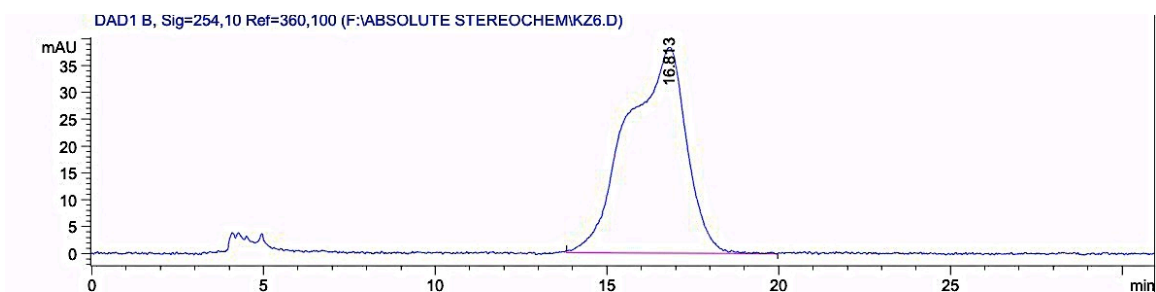
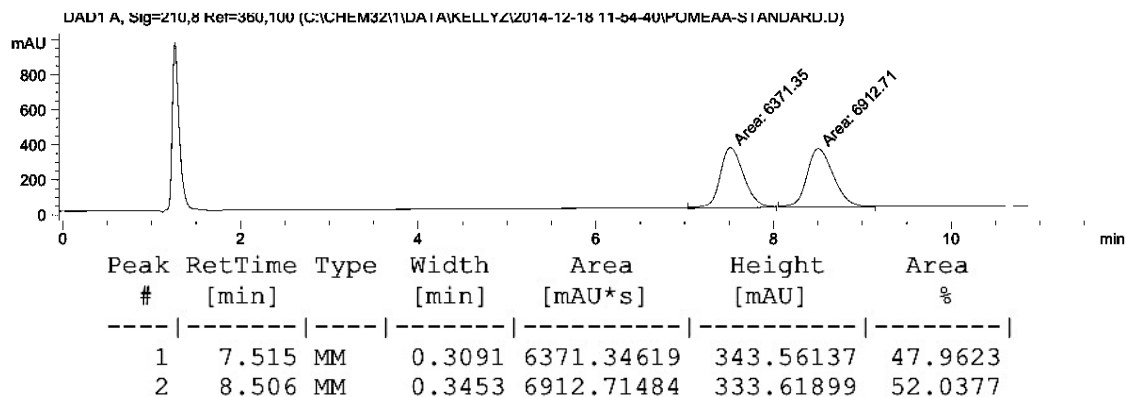


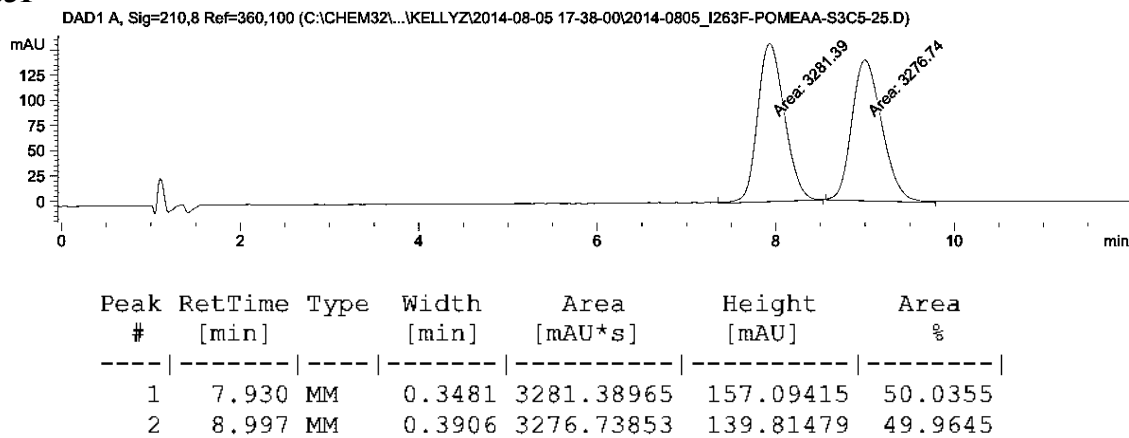
Figure S15. Enantioselectivity for enzyme-catalyzed formation of amido-alcohol 2.

Selectivity was assessed by SFC using Chiralpak AS-H column with 25% isopropanol : 75% supercritical CO₂ mobile phase. Representative chromatograms are shown below.

Racemic synthetic standard



P-I263F



P-I263F-A328V-L437V

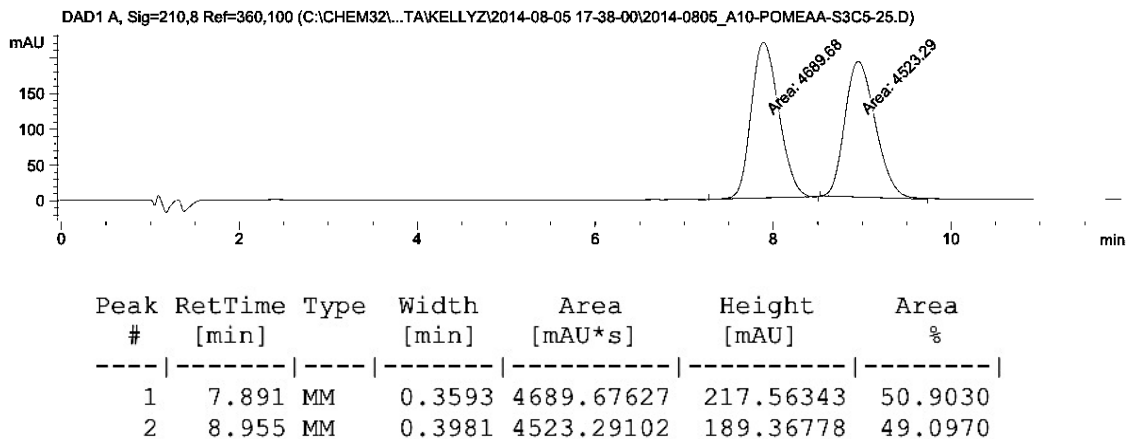
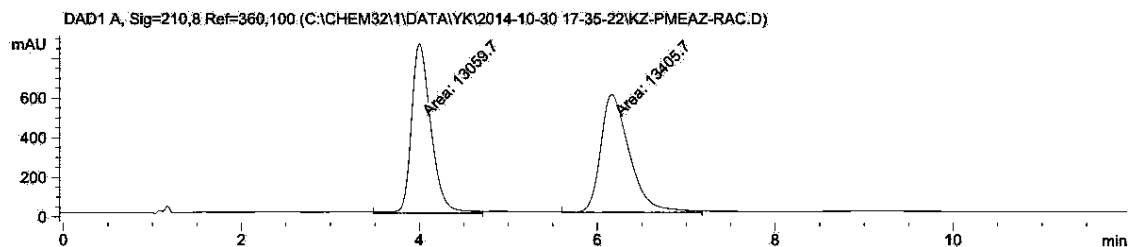


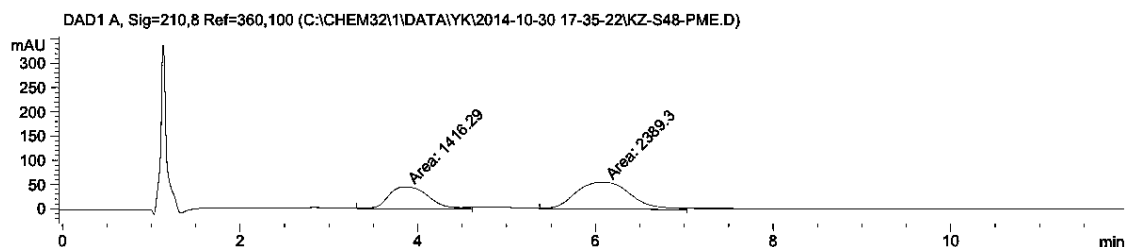
Figure S16. Enantioselectivity for enzyme-catalyzed formation of aziridine 4.
 Selectivity was assessed by SFC using Chiralpak OB-H column with 20% isopropanol : 80% supercritical CO₂ mobile phase. Representative chromatograms are shown below.

Racemic synthetic standard



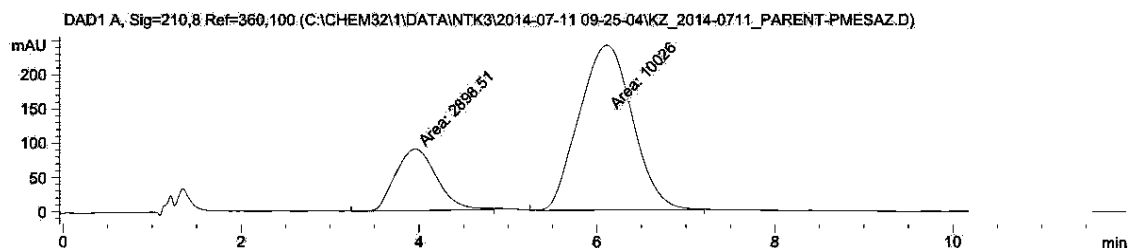
Peak #	RetTime [min]	Type	Width [min]	Area [mAU*s]	Height [mAU]	Area %
1	4.000	MM	0.2545	1.30597e4	855.30292	49.3464
2	6.162	MM	0.3757	1.34057e4	594.68988	50.6536

P411_{BM3}-CIS T438S (P)



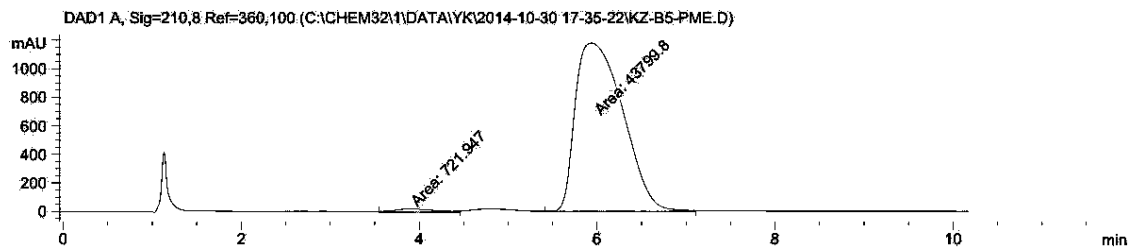
Peak #	RetTime [min]	Type	Width [min]	Area [mAU*s]	Height [mAU]	Area %
1	3.857	MM	0.5209	1416.29333	45.31232	37.2161
2	6.084	MM	0.7149	2389.29932	55.70283	62.7839

P-I263F



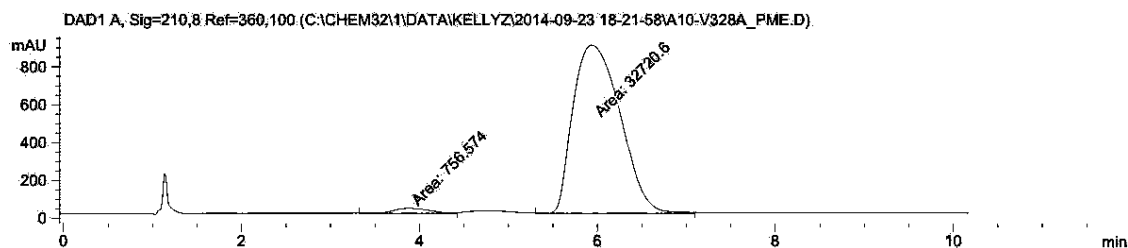
Peak #	RetTime [min]	Type	Width [min]	Area [mAU*s]	Height [mAU]	Area %
1	3.960	MM	0.5373	2898.51050	89.90318	22.4264
2	6.110	MM	0.6936	1.00260e4	240.92017	77.5736

P-I263F-A328V



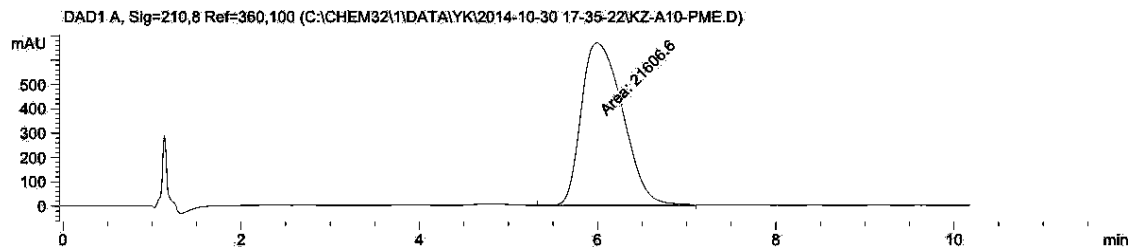
Peak #	RetTime [min]	Type	Width [min]	Area [mAU*s]	Height [mAU]	Area %
1	3.869	MM	0.5473	721.94702	21.98478	1.6216
2	5.935	MM	0.6196	4.37998e4	1178.10986	98.3784

P-I263F-L437V



Peak #	RetTime [min]	Type	Width [min]	Area [mAU*s]	Height [mAU]	Area %
1	3.876	MM	0.4836	756.57367	26.07187	2.2600
2	5.934	MM	0.6139	3.27206e4	888.33771	97.7400

P-I263F-A328V-L437V

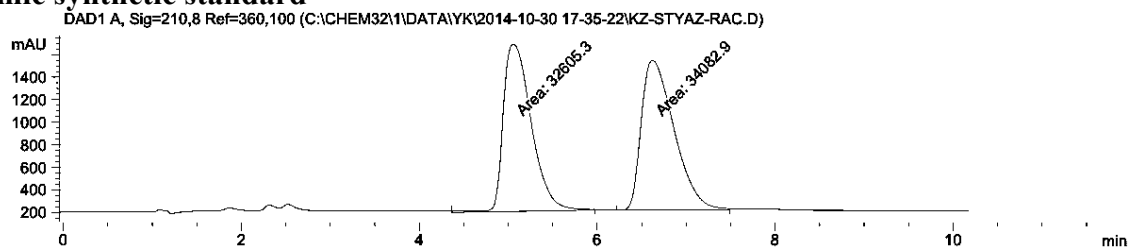


Peak #	RetTime [min]	Type	Width [min]	Area [mAU*s]	Height [mAU]	Area %
1	5.992	MM	0.5394	2.16066e4	667.58752	100.0000

Figure S17. Enantioselectivity for enzyme-catalyzed formation of 6.

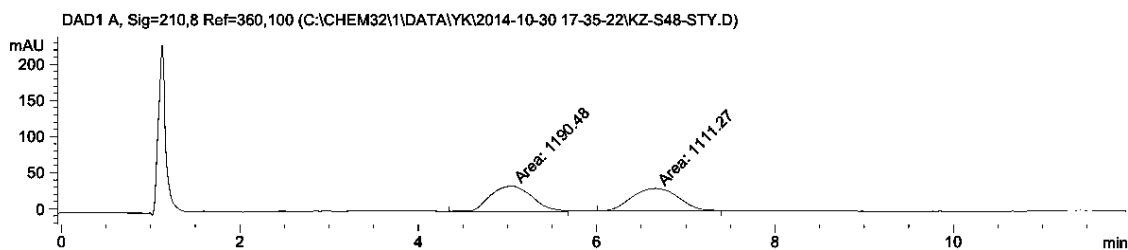
Selectivity was assessed by SFC using Chiralpak OB-H column with 15% isopropanol : 85% supercritical CO₂ mobile phase. Representative chromatograms are shown below.

Racemic synthetic standard



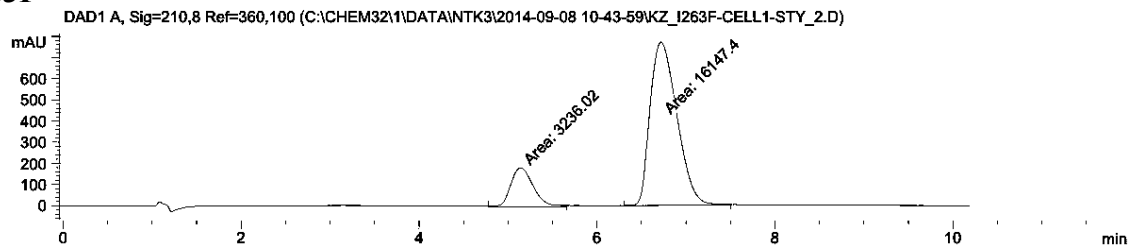
Peak #	RetTime [min]	Type	Width [min]	Area [mAU*s]	Height [mAU]	Area %
1	5.057	MM	0.3659	3.26053e4	1485.14514	48.8922
2	6.622	MM	0.4271	3.40829e4	1329.99841	51.1078

P411_{BM3}-CIS T438S (P)



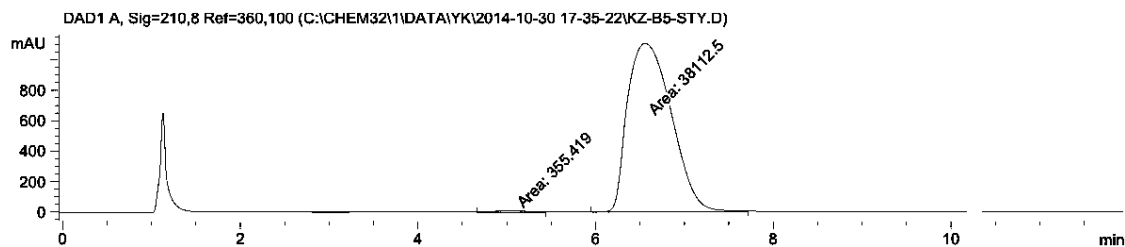
Peak #	RetTime [min]	Type	Width [min]	Area [mAU*s]	Height [mAU]	Area %
1	5.040	MM	0.5540	1190.47607	35.81605	51.7206
2	6.651	MM	0.6016	1111.27014	30.78856	48.2794

P-I263F



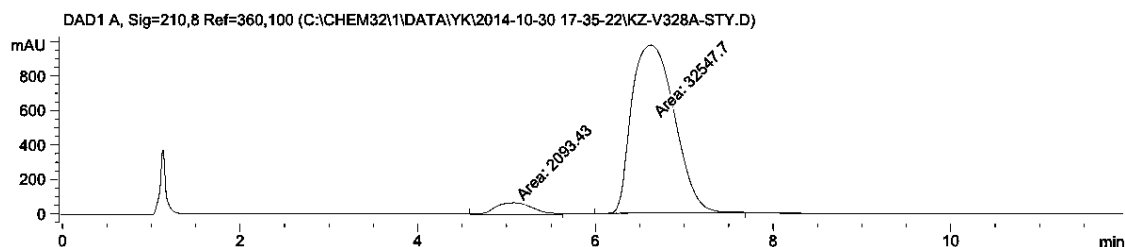
Peak #	RetTime [min]	Type	Width [min]	Area [mAU*s]	Height [mAU]	Area %
1	5.140	MM	0.2953	3236.01807	182.66165	16.6948
2	6.720	MM	0.3487	1.61474e4	771.80231	83.3052

P-I263F-A328V



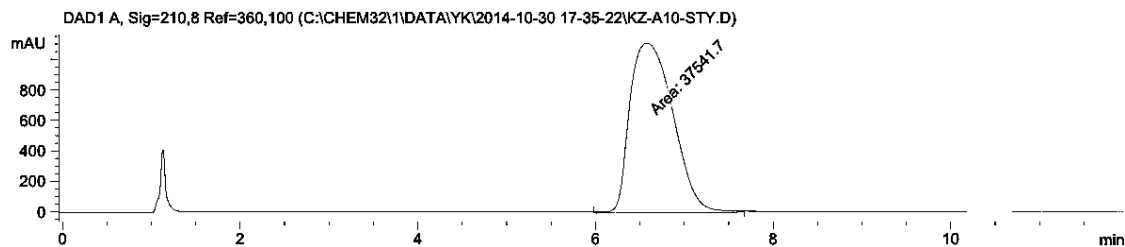
Peak #	RetTime [min]	Type	Width [min]	Area [mAU*s]	Height [mAU]	Area %
1	5.077	MM	0.5269	355.41898	11.24200	0.9239
2	6.558	MM	0.5721	3.81125e4	1110.29065	99.0761

P-I263F-L437V



Peak #	RetTime [min]	Type	Width [min]	Area [mAU*s]	Height [mAU]	Area %
1	5.078	MM	0.5042	2093.43091	69.20262	6.0432
2	6.624	MM	0.5566	3.25477e4	974.59937	93.9568

P-I263F-A328V-L437V

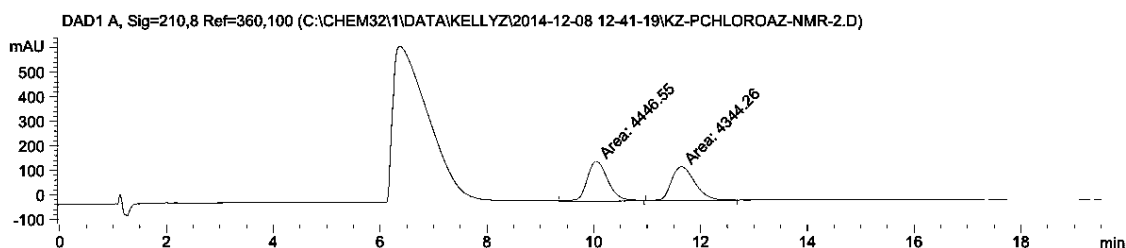


Peak #	RetTime [min]	Type	Width [min]	Area [mAU*s]	Height [mAU]	Area %
1	6.576	MM	0.5627	3.75417e4	1112.00940	100.0000

Figure S18. Enantioselectivity for enzyme-catalyzed formation of S2-S7.

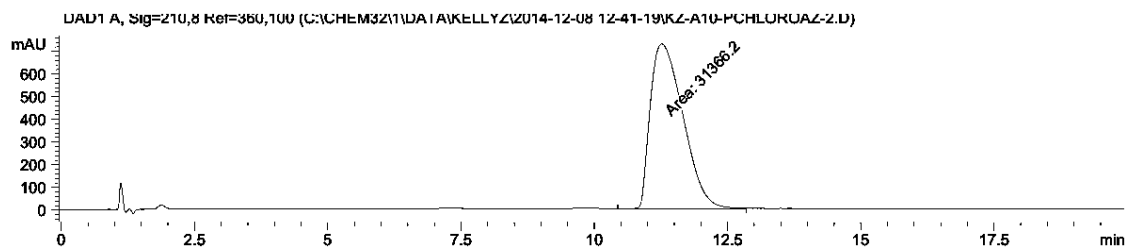
Selectivity was assessed by SFC using either chiral AS-H (S2, S6, S7) or OB-H column (S3, S4, S5) with isopropanol and supercritical CO₂ as mobile phase. Representative chromatograms are shown below.

Racemic synthetic standard S2



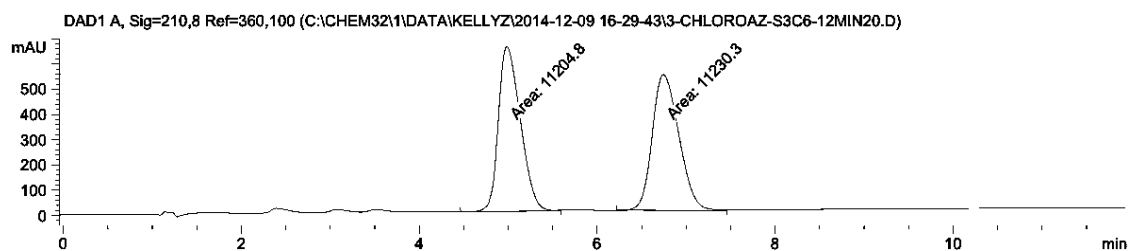
Peak #	RetTime [min]	Type	Width [min]	Area [mAU*s]	Height [mAU]	Area %
1	10.048	MM	0.4545	4446.55078	163.06299	50.5818
2	11.641	MM	0.5222	4344.26123	138.65178	49.4182

P-I263F-A328V-L437V produced S2



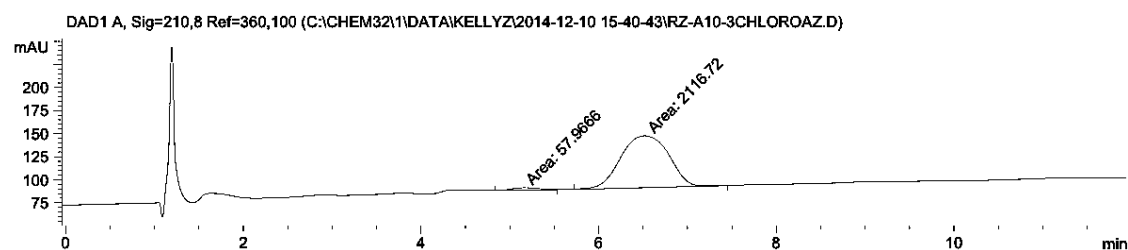
Peak #	RetTime [min]	Type	Width [min]	Area [mAU*s]	Height [mAU]	Area %
1	11.265	MM	0.7168	3.13662e4	729.26678	100.0000

Racemic synthetic standard S3



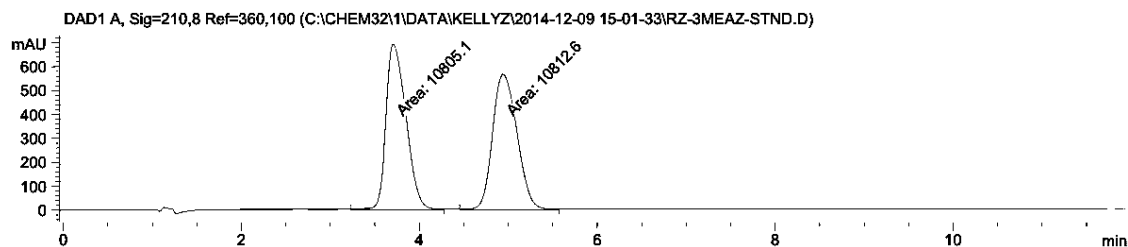
Peak #	RetTime [min]	Type	Width [min]	Area [mAU*s]	Height [mAU]	Area %
1	4.985	MM	0.2862	1.12048e4	652.60254	49.9432
2	6.745	MM	0.3482	1.12303e4	537.54370	50.0568

P-I263F-A328V-L437V produced S3



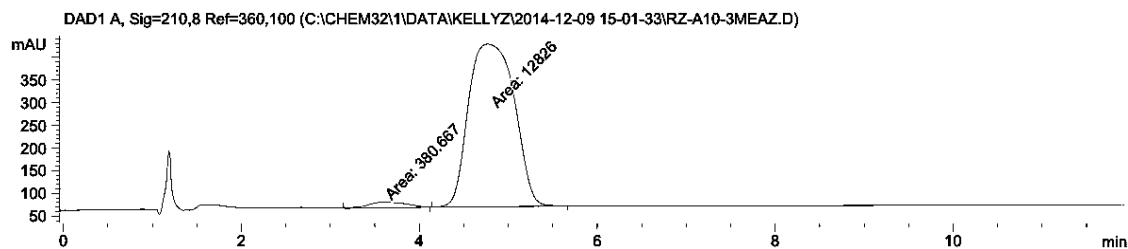
Peak #	RetTime [min]	Type	Width [min]	Area [mAU*s]	Height [mAU]	Area %
1	5.145	MM	0.3705	57.96660	2.60781	2.6655
2	6.516	MM	0.6276	2116.71973	56.21136	97.3345

Racemic synthetic standard S4



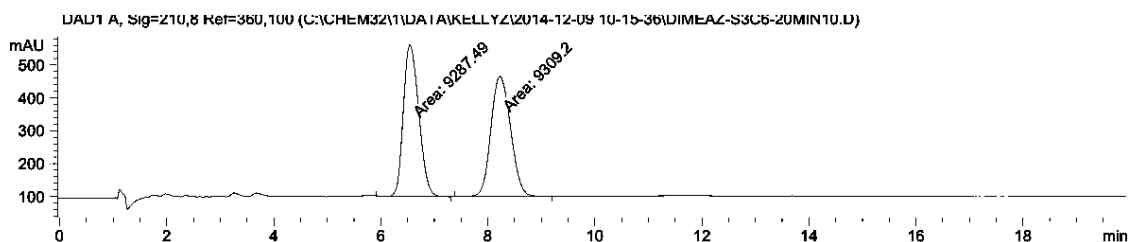
Peak #	RetTime [min]	Type	Width [min]	Area [mAU*s]	Height [mAU]	Area %
1	3.708	MM	0.2602	1.08051e4	692.21600	49.9826
2	4.942	MM	0.3186	1.08126e4	565.55908	50.0174

P-I263F-A328V-L437V produced S4



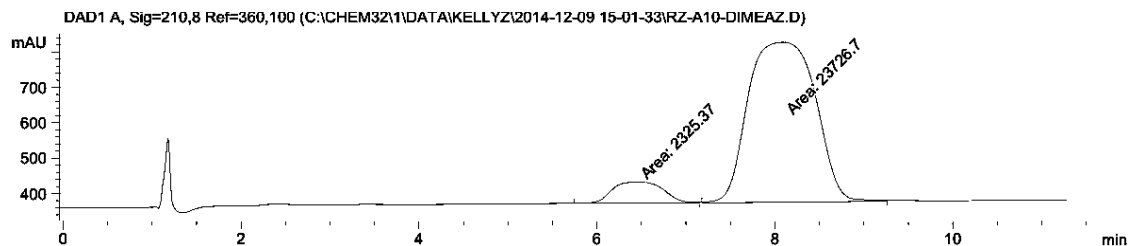
Peak #	RetTime [min]	Type	Width [min]	Area [mAU*s]	Height [mAU]	Area %
1	3.579	MM	0.5097	380.66705	12.44634	2.8824
2	4.770	MM	0.5976	1.28260e4	357.67941	97.1176

Racemic synthetic standard S5



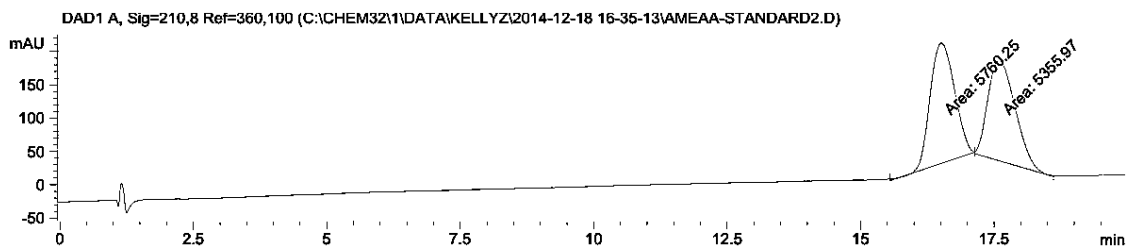
Peak #	RetTime [min]	Type	Width [min]	Area [mAU*s]	Height [mAU]	Area %
1	6.545	MM	0.3348	9287.48535	462.29697	49.9416
2	8.226	MM	0.4250	9309.19922	365.07251	50.0584

P-I263F-A328V-L437V produced S5



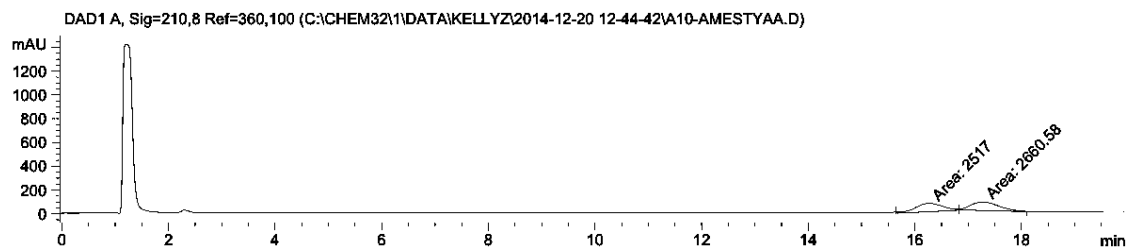
Peak #	RetTime [min]	Type	Width [min]	Area [mAU*s]	Height [mAU]	Area %
1	6.455	MM	0.6568	2325.36816	59.01160	8.9258
2	8.093	MM	0.8759	2.37267e4	451.45123	91.0742

Racemic synthetic standard S6



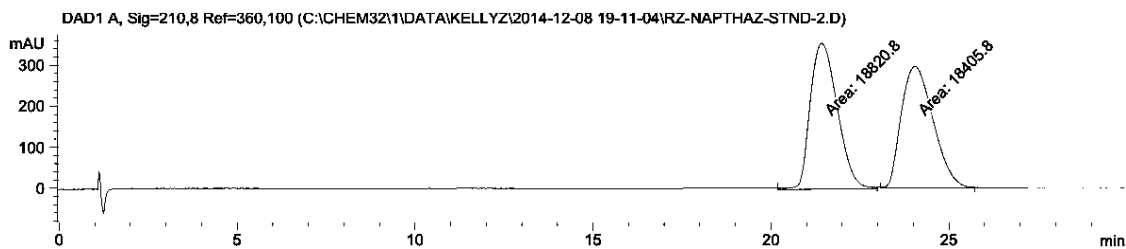
Peak #	RetTime [min]	Type	Width [min]	Area [mAU*s]	Height [mAU]	Area %
1	16.511	MM	0.5311	5760.24756	180.76260	51.8184
2	17.607	MM	0.5928	5355.97217	150.58235	48.1816

P-I263F-A328V-L437V produced S6



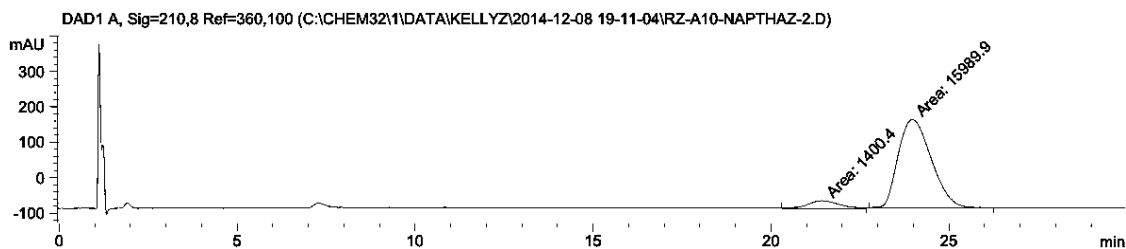
Peak #	RetTime [min]	Type	Width [min]	Area [mAU*s]	Height [mAU]	Area %
1	16.265	MM	0.5942	2517.00049	70.60035	48.6135
2	17.276	MM	0.6129	2660.57593	72.35230	51.3865

Racemic synthetic standard S7



Peak #	RetTime [min]	Type	Width [min]	Area [mAU*s]	Height [mAU]	Area %
1	21.429	MM	0.8822	1.88208e4	355.55453	50.5574
2	24.049	MM	1.0350	1.84058e4	296.38309	49.4426

P-I263F-A328V-L437V produced S7

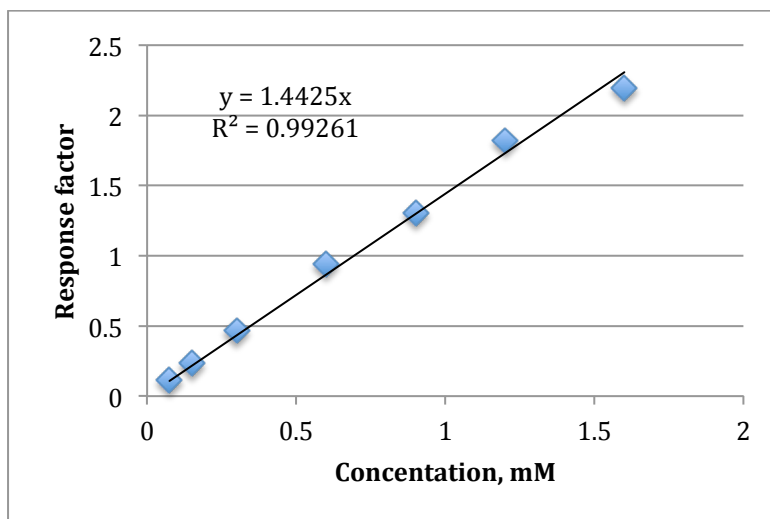


Peak #	RetTime [min]	Type	Width [min]	Area [mAU*s]	Height [mAU]	Area %
1	21.465	MM	1.0441	1400.40186	22.35329	8.0528
2	23.976	MM	1.0731	1.59899e4	248.33498	91.9472

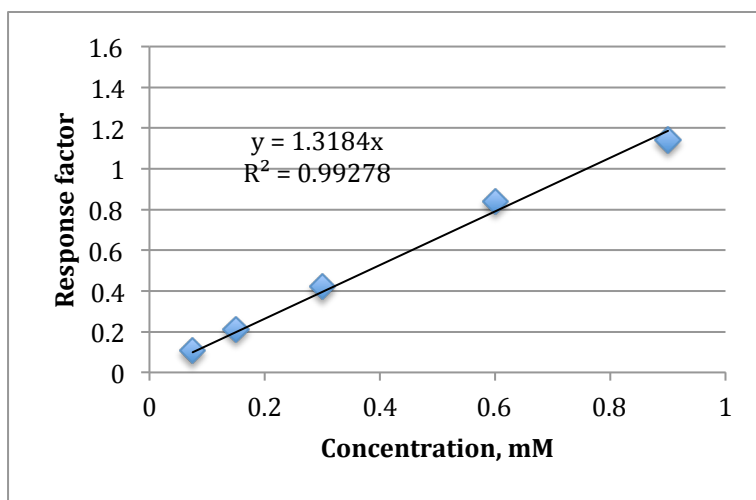
Figure S19: Calibration curves for aziridine and amido-alcohol products

Calibration curves show response factor (the ratio of product area to internal standard area, y-axis) and concentration of product (x-axis).

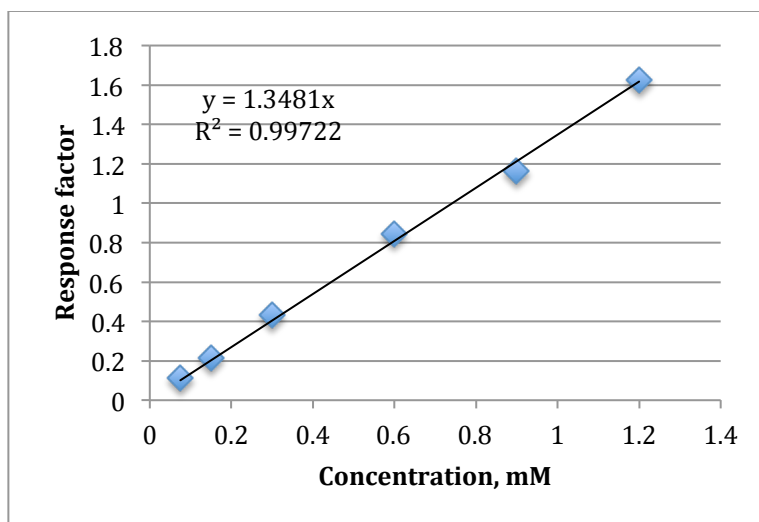
Amido-alcohol 2.



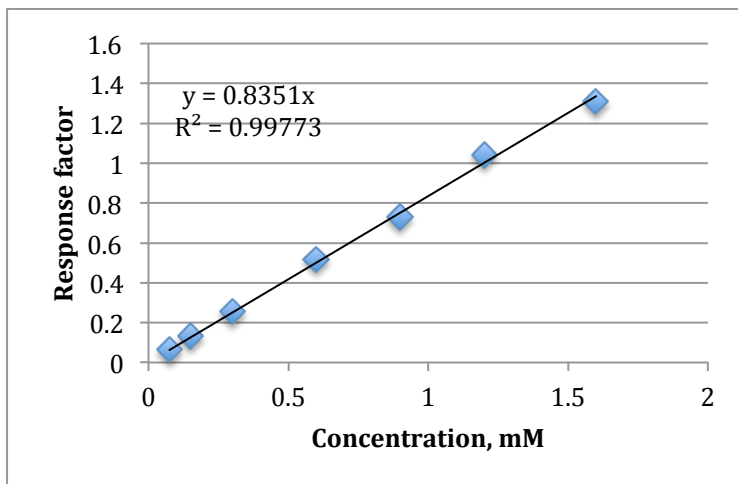
Aziridines 4 and S4. Calibration curve constructed using 4.



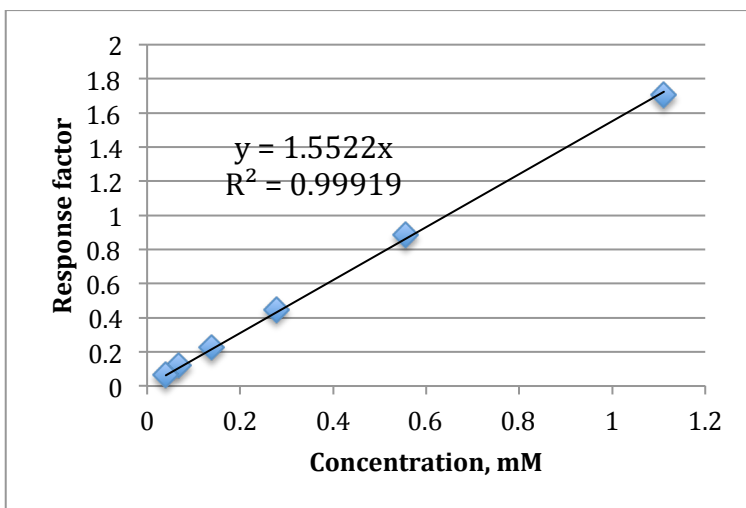
Aziridine 6.



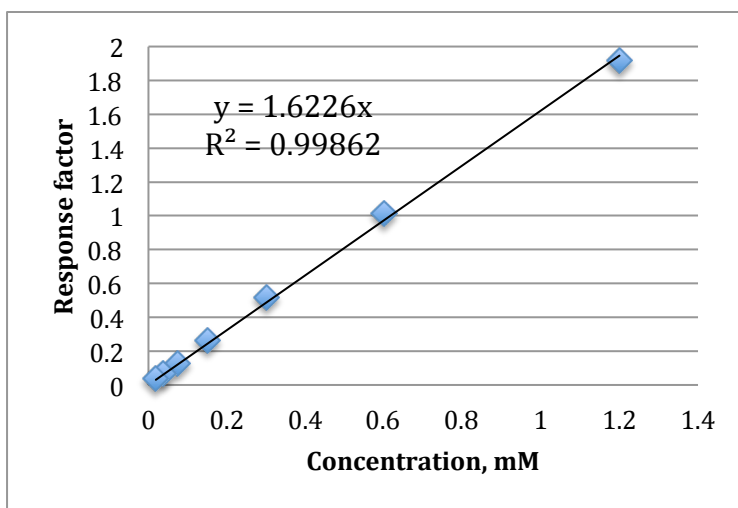
Sulfonamide 7.



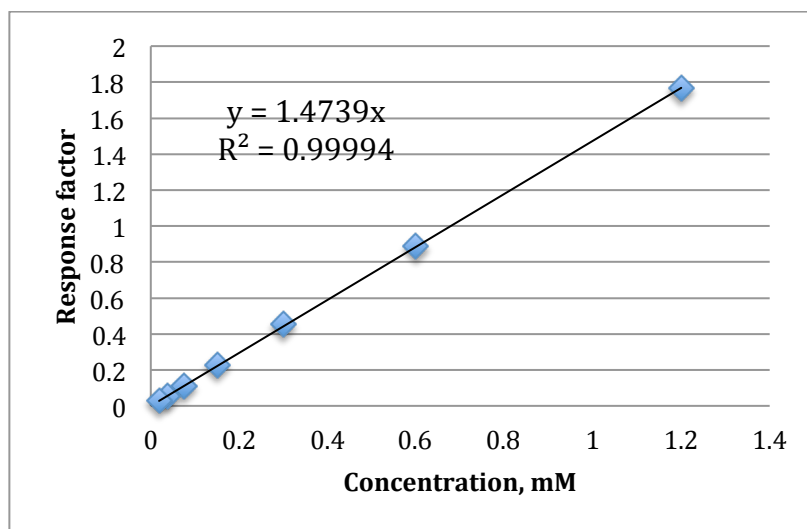
Aziridines S2 and S3. Calibration curve constructed using S2.



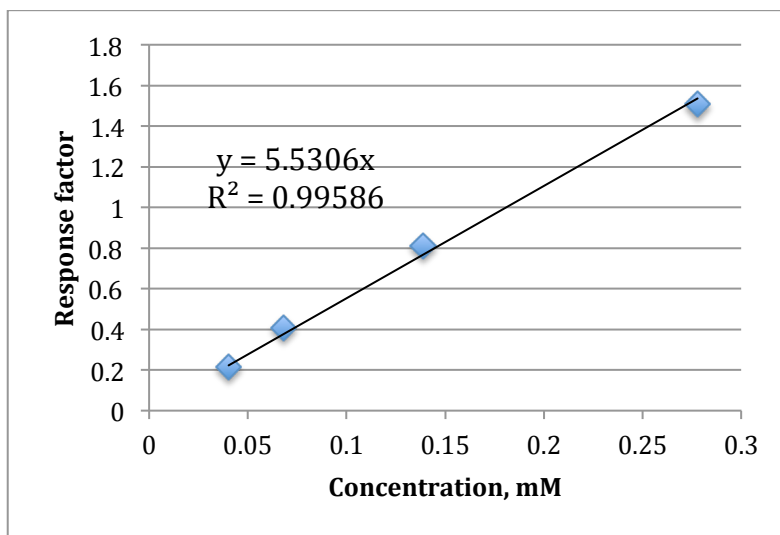
Aziridine S5.



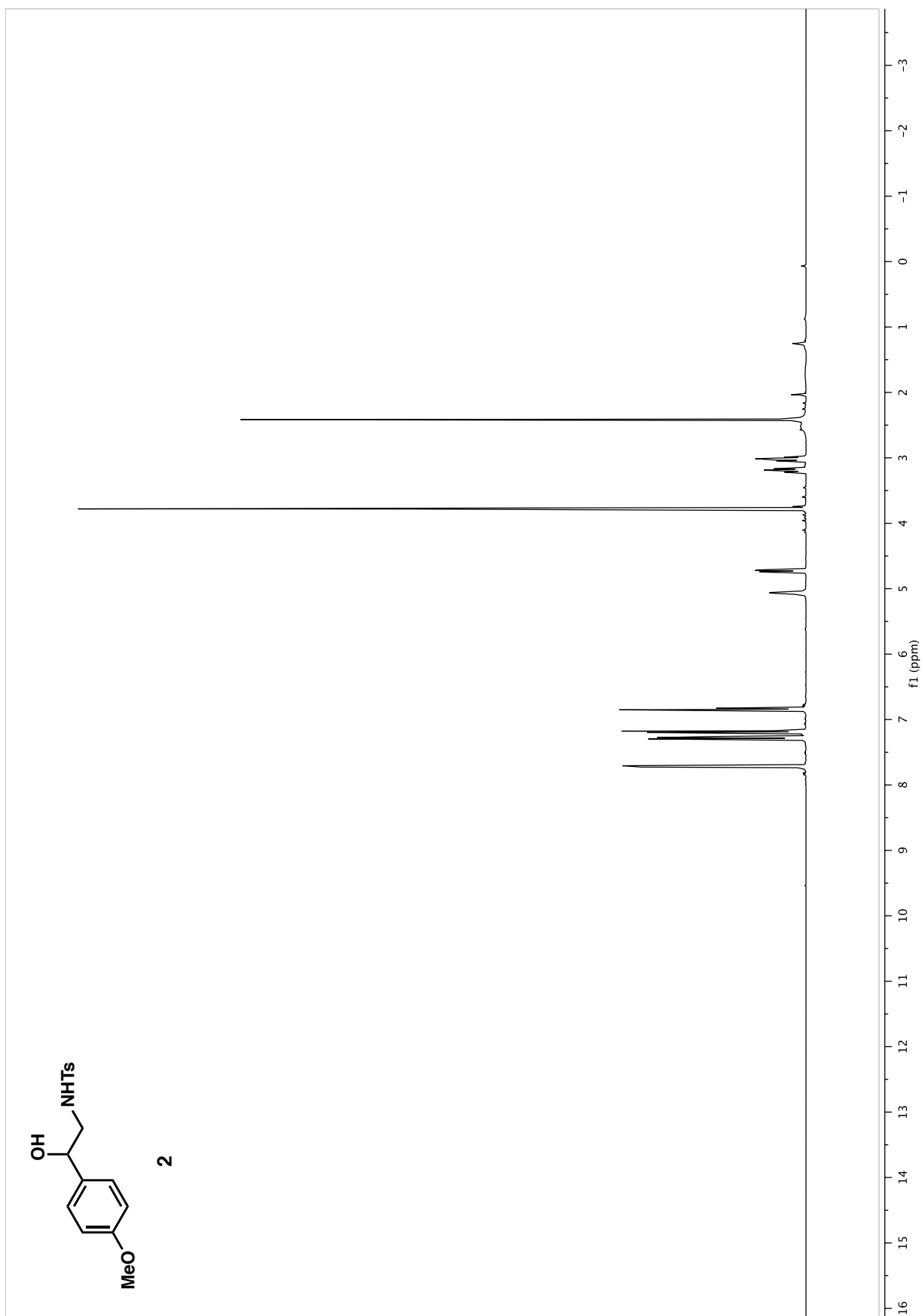
Amido-alcohol S6.

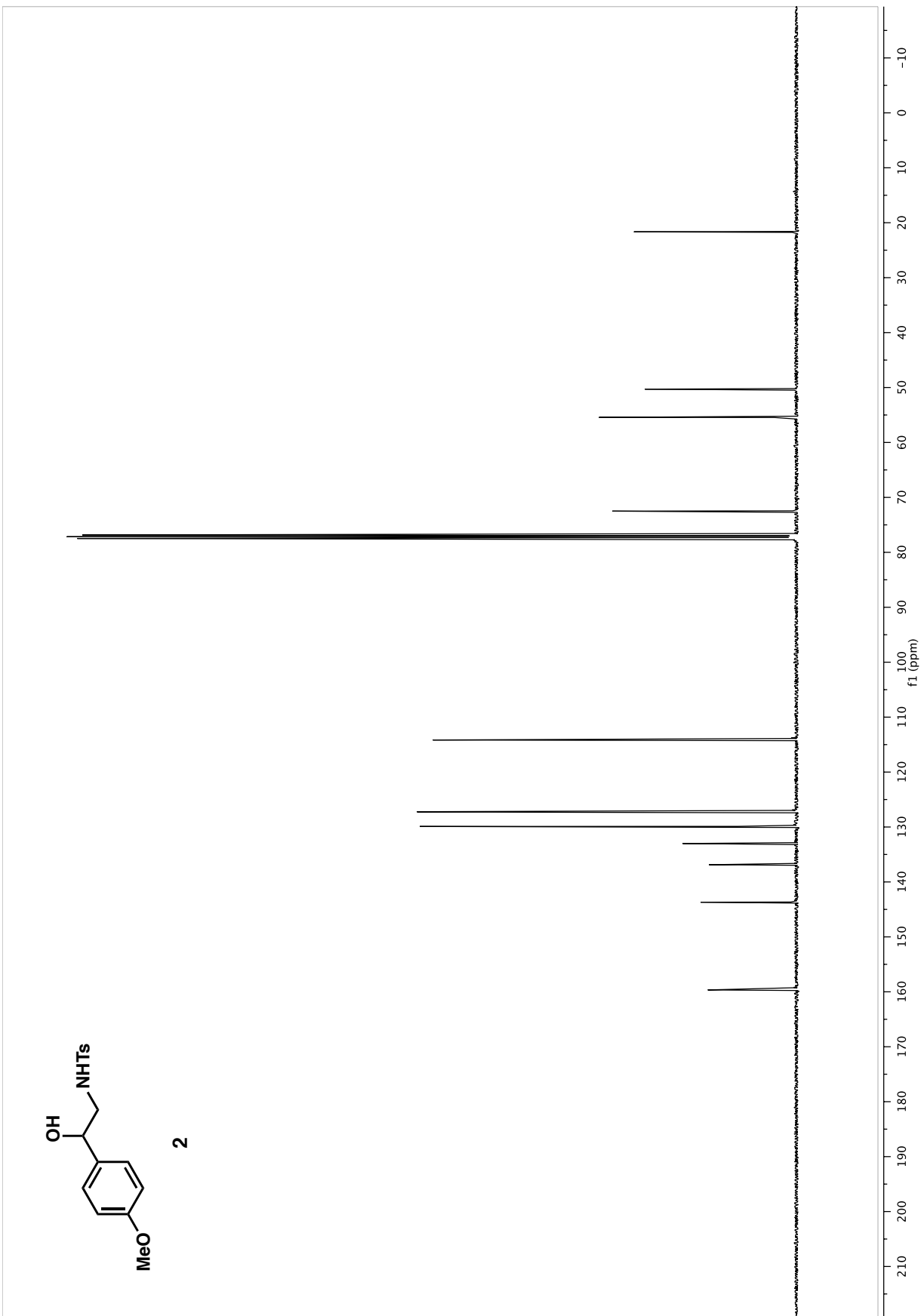


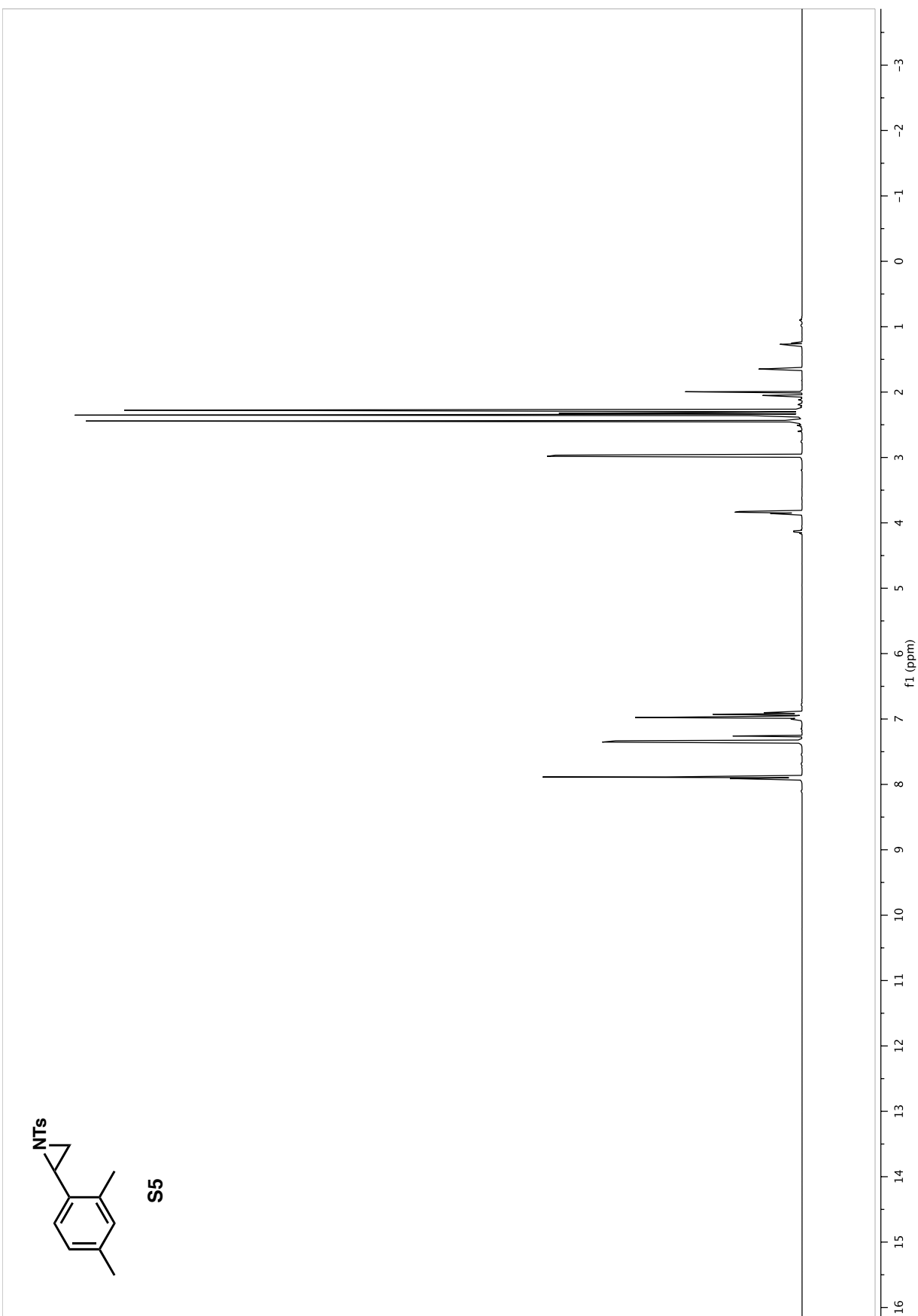
Aziridine S7.

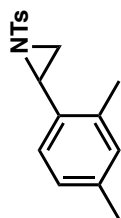


^1H (400 MHz, CDCl_3) and ^{13}C (101 MHz, CDCl_3) spectra

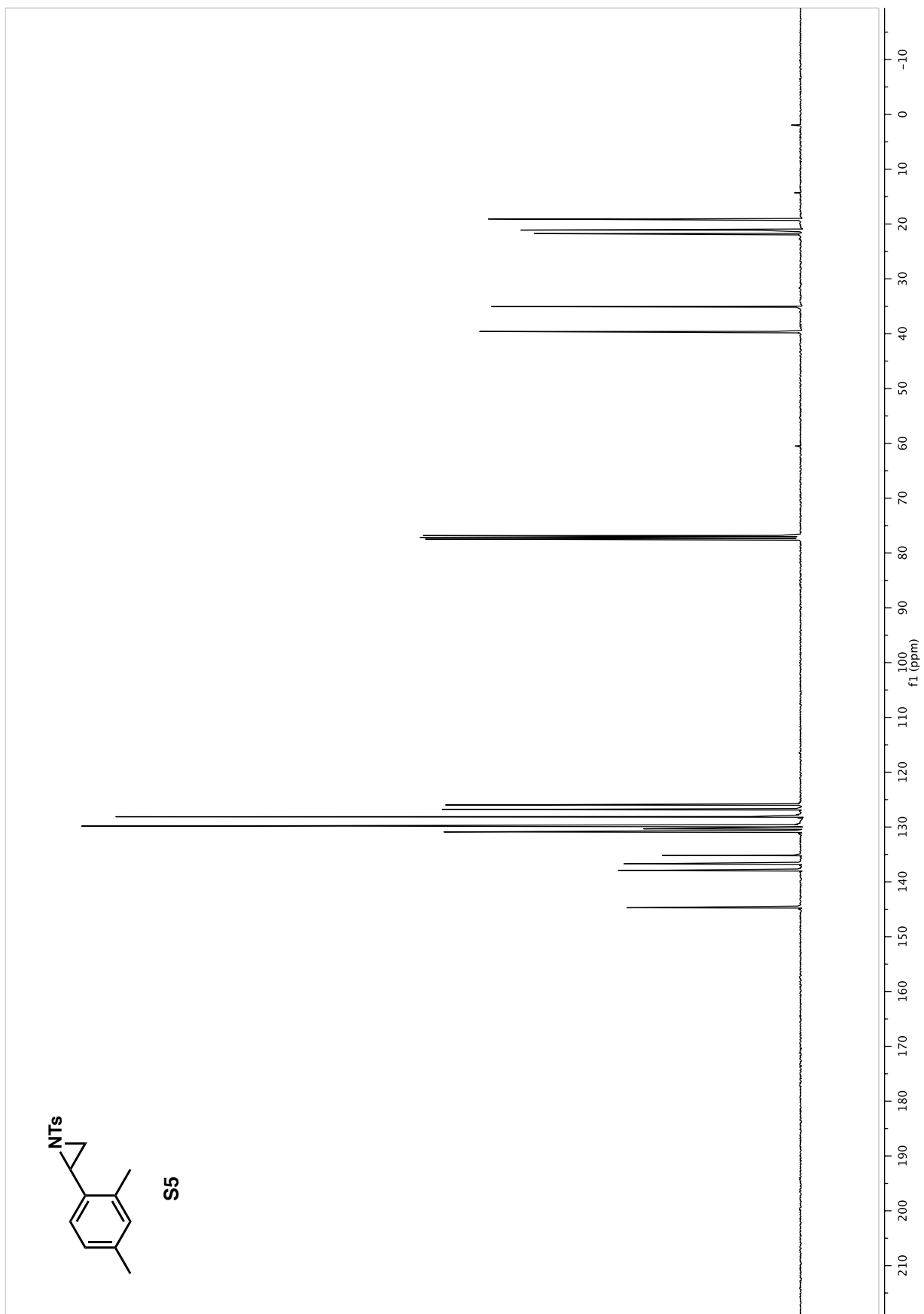


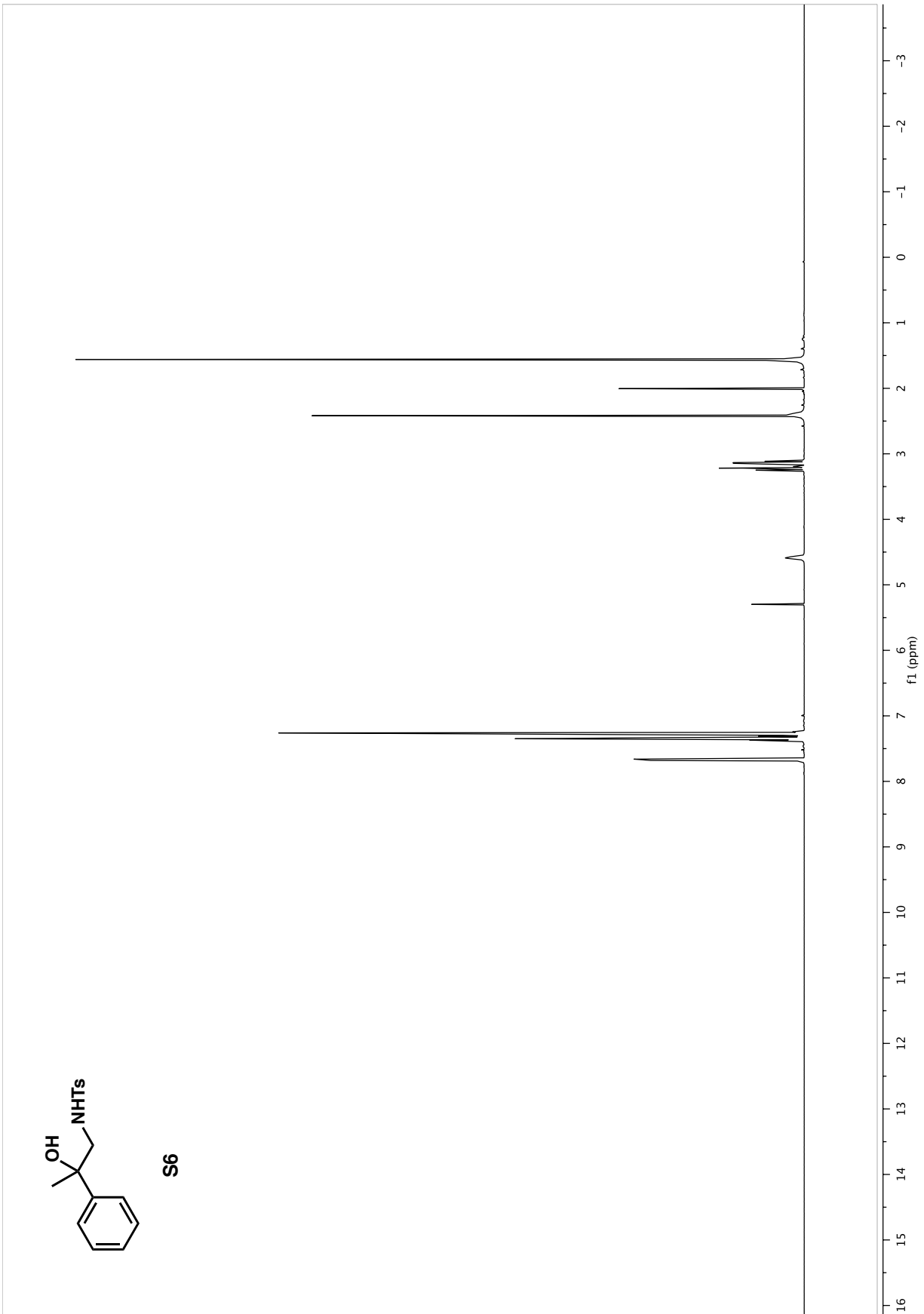


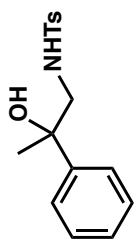




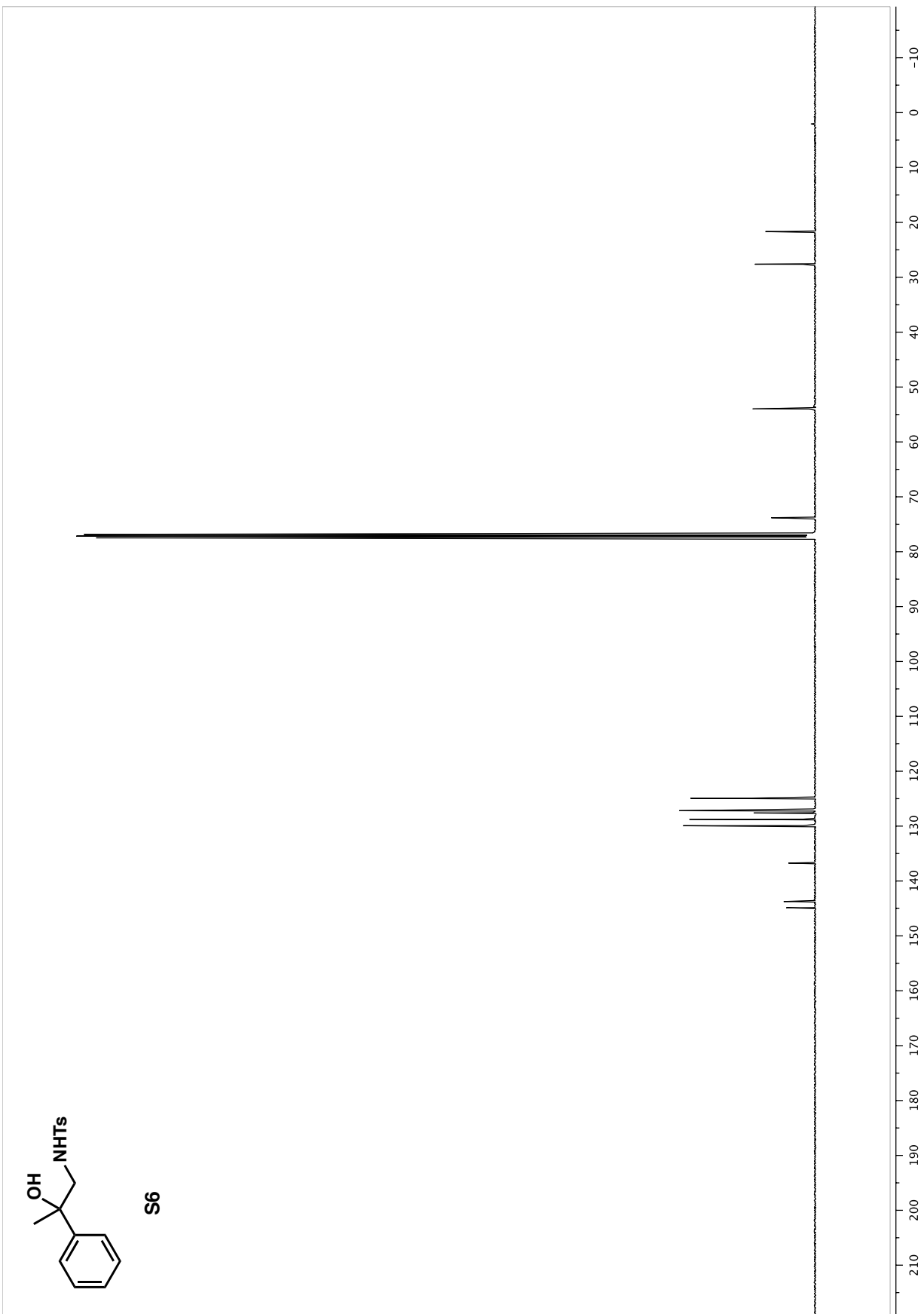
S5







S6



References

- S1. Srinivas, B.; Kumar, V.P.; Sridhar, R.; Surendra, K.; Nageswar, Y.V.D; Rao, K.R. *J. Mol. Catal. A: Chem.* **2007**, *261*, 1–5.
- S2. Ando, T.; Kano, D.; Minakata, S.; Ryu, I; Komatsu, M. *Tetrahedron* **1998**, *54*, 13485–13494
- S3. a) Omura T.; Sato, R. *J. Biol. Chem.* **1964**, *239*, 2370–2378; b) Vatsis, K.P.; Peng, H.M.; Coon, M.J. *J. Inorg. Biochem.* **2002**, *91*, 542-553.
- S4. Berry, E. A.; Trumpower, B. L. *Anal. Biochem.* **1987**, *161*, 1–15.
- S5. Coelho, P. S.; Brustad, E. M.; Kannan, A.; Arnold, F. H. *Science* **2013**, *339*, 307–310.
- S6. Kille, S.; Acevedo-Rocha, C.G.; Parra, L.P.; Zhang, Z.G.; Opperman, D.J.; Reetz, M.T.; Acevedo, J.P., *ACS Synth. Biol.* **2013**, *2*, 83–92.
- S7. Takeda Y.; Ikeda, Y.; Kuroda, A.; Tanaka, S.; Minakata, S. *J. Am. Chem. Soc.* **2014**, *136*, 8544-8547.
- S8. a) Alonso, D.A.; Andersson, P.G.; *J. Org. Chem.* **1998**, *63*, 9455-9461; b) Wang, X.; Ding, K. *Chem. Eur. J.* **2006**, *12*, 4568-4575.
- S9. Farwell, C.C. et al. *J. Am. Chem. Soc.* **2014**, *136*, 8766–8771
- S10. a) Huang, C. Y.; Doyle, A. G. *J. Am. Chem. Soc.* **2012**, *134*, 9541–9544. b) Kiyokawa, K.; Kosaka, T.; Minakata, S., *Org. Lett.* **2013**, *15*, 4858–4861; c) Evans. D. A.; Faul, M. M.; Bilodeau, M. T. *J. Am. Chem. Soc.* **1994**, *116*, 2742–2753
- S11. Craig II, R.A.; O'Connor, N.R.; Goldberg, A.F.G.; Stoltz, B.M. *Chem. Eur. J.* **2014**, *20*, 4806 – 4813.
- S12. Gao, G.Y.; Harden, J.D.; Zhang, X.P. *Org. Lett.* **2005**, *7*, 3191–3193.
- S13. Hyster, T.K.; Farwell, C.C.; Buller, A.R.; McIntosh, J.A.; Arnold. F.H. *J. Am. Chem. Soc.* **2014**, *136*, 15505–15509.
- S14. Heel, T.; McIntosh, J.A.; Dodani, S.C.; Meyerowitz, J.T.; Arnold, F.H. *ChemBioChem.* **2014**, *15*, 2556–2562.